

MSc Thesis

**System Component Modelling of Electric
Vehicles and Charging Infrastructure**

Author: Emanuel Tsakmakis

Session: July 2013

**University: Universitat Politècnica de Catalunya.
Barcelona Tech.**

**MSc Program: Environomical Pathways for
Sustainable Energy Systems – SELECT**

Supervisors:

Principal supervisor: Prof. Andreas Sumper

Industrial supervisor: MSc Fabian Möhrke



Escola Tècnica Superior
d'Enginyeria Industrial de Barcelona

UNIVERSITAT POLITÈCNICA DE CATALUNYA



MSc SELECT is a cooperation between

Abstract

The objective of this research is to develop a model for the electrical components that are involved in charging and discharging of an electric vehicle (EV). This will enable testing different energy management strategies that improve energy efficiency, battery lifetime, and energy availability. Furthermore, the model will enable the investigation of vehicle to grid (V2G), thermal preconditioning of vehicles, and an economic analysis and optimization.

In order to achieve the above goals, the effects that determine the performance of the infrastructure, rectifier, and battery are investigated and included as a second step in a parameterized model. Implementing an open loop control enables sample times of one minute and, by simplifying the process for a low runtime, multiple EVs can be included in the simulation of a smart grid. The structure is designed in a way as to support both uncontrolled and controlled charging with variable charging power and variable charging current.

For the battery, a simple model approach was developed that limits the computational complexity and the effort for parameterization. It was found that the energy management of an electric vehicle is a complex process with battery handling being a key issue. The performance is dependent on various parameters that involve battery temperature, depth of discharge, and charge and discharge rates.

Acknowledgements

I would like to express my gratitude to my supervisors Prof. Andreas Sumper and Fabian Möhrke for the useful comments, remarks, and guidance through the learning process of this master thesis. Furthermore, I would like to thank the Reiner Lemoine Institute for creating a stimulating and motivating environment.

I would also like to thank the SELECT program for providing this life changing experience, financial support, and the inspiration.

Finally, I would like to thank my family and friends for their continuous support throughout the course of the thesis and keeping both my soul and my body healthy.

Table of Contents

Abstract.....	i
Acknowledgements	ii
Table of Contents.....	iii
List of Tables.....	v
List of Figures.....	vi
List of Abbreviations	vii
List of Units	vii
1. Introduction.....	1
1.1. Structure of the Thesis	2
2. Electric Components	3
2.1. Charging Station and Grid Connection.....	3
2.2. Battery.....	5
2.2.1. Performance Indicators.....	6
2.2.2. Temperature and Number of Cycles.....	8
2.2.3. Depth of Discharge and Number of Cycles	10
2.2.4. Charge Discharge Current Rates and Number of Cycles	10
2.3. Auxiliaries in Cars	11
3. Modelling Approach.....	13
3.1. Simulation Requirements and Validity.....	13
3.2. Modelling Basics.....	14
3.3. Battery Models.....	15
3.3.1. Physical or Electrochemical Models.....	15
3.3.2. Empirical or Phenomenological Models	15
3.3.3. Electric Circuit Models	16
4. Simulation of Charging and Discharging Process.....	18
4.1. Internal Structure.....	19
4.2. Charging Infrastructure and Charger	21
4.3. Electric Vehicle Battery Simulation	22

4.3.1.	Assumptions.....	22
4.3.2.	Implementation of the Control.....	24
4.3.3.	Solving the Equivalent Circuit.....	26
4.4.	Power Allocation.....	27
5.	Verification and Results.....	29
5.1.	Verification of the Battery Model.....	29
5.2.	Verification of the Control Strategies.....	31
5.2.1.	Controller Stage 1: Power and Current Control.....	31
5.2.2.	Controller Stage 2: Capacity and Voltage Control.....	32
5.3.	Test Case.....	33
5.4.	Review of the simulation tool.....	36
6.	Conclusion.....	38
6.1.	Further Work.....	39
	References.....	41
	Appendix A: Glossary for the Term Capacity.....	44

List of Tables

Table 1: Specifications of the maximum power demand according to industrial specifications [9]

Table 2: Effects of external and operational parameter on entities of the electric circuit model

Table 3: Overview of the influence of operational conditions on the performance of EV-batteries

Table 4: Energy available for discharging batteries at different temperatures based on datasheet [15]

Table 5: Energy available during discharging at different CRs based on datasheet [15]

Table 6: Disadvantages and advantages of the model of Trembley et al. [25]

Table 7: Summary of the test case simulation

List of Figures

Figure 1: Self-discharge of a battery over a year [14]

Figure 2: a) charging efficiency, b) energy efficiency and c) resistance (vertical axis) depending on the temperature (bottom left axis) and the SOC (bottom right axis) [13]

Figure 3: Influence of temperature on a) available energy and b) capacity based on [15]

Figure 4: Life expectancy for different DOD rates [17]

Figure 5: Influence of CR on available energy based on [15]

Figure 6: Bi-directional charger performance

Figure 7: Layout of the model for controlled charging of the electric vehicle

Figure 8: The flowchart of the electric vehicle and charging infrastructure model

Figure 9: Transmission losses for single phase and three phase transmission

Figure 10: The performance of the bi-directional converter

Figure 11: Equivalent circuit model of battery cell

Figure 12: Graphical explanation of determining the open circuit voltage from a discharge curve [15]

Figure 13: Layout of the controller stage 1

Figure 14: Controller stage 2

Figure 15: The limitation of the power for solving the equivalent circuit.

Figure 16: Definition of the power flows

Figure 17: Discharging behaviour of the model compared with datasheet information

Figure 18: Charging behaviour of the model compared with datasheet information

Figure 19: Behaviour of system for variable power control

Figure 20: Behaviour constant current control for a constant current of 0.53 A (0.1C)

Figure 21: Behaviour of the battery for the controller stage 2 based on capacity

Figure 22: Behaviour of the battery for the controller stage 2 based on voltage

Figure 23: Performance of the EV

Figure 24: Internal states of the model for the test case

List of Abbreviations

AEV: All electric vehicle

CCCV: Constant current constant voltage

CR: Charge and discharge rate

CN: Number of cycles

DOD: Depth-of-discharge

EV: Electric vehicle

HEV: Hybrid electric vehicle

HV: High voltage

ICE: Internal combustion engine

OCV: Open circuit voltage

OSS: On-board supply system

PHEV: Plug-in hybrid electric vehicle

SOC: State of charge

V2G: Vehicle to grid

List of Units

W: Watt

V: Volt

A: Ampere

Ah: Ampere hours

km: kilometre

mOhm: Milliohm

1. Introduction

Road transport contributes to approximately one-fifth of the EU's total carbon dioxide (CO₂) emissions. CO₂ is one of the most prevalent greenhouse gases, and CO₂ emissions from road transport alone increased by nearly 23 % between 1990 and 2010, and could have been even higher without the economic crisis [1]. Cars with different degrees of hybridization are a solution because they can have up to 6 times more fuel economy relative to vehicles powered solely by conventional internal combustion engines (ICEs) [2]. Furthermore, hybrid vehicles can offer economic benefits through the integration of electric mobility in a smart grid with a high share of intermittent generation by shifting demand to off-peak hours and using the car battery as a storage device in vehicle to grid (V2G) applications. This is achieved by optimized and controlled charging and the usage of the electric vehicle (EV) battery as an integrated part of the electric grid.

It is expected that plug-in hybrid electric vehicles (PHEV) will soon become cost effective and that higher investment costs for the battery will amortize over the lifetime of the vehicle. A market study by A. T. Kearney forecasts that by the year 2025 PHEVs and all electric vehicles (AEVs) together will contribute a share of 30% of the compact car market in Europe. Only 35% of powertrain configurations will be based solely on an internal combustion engine [3]. Still, there are obstacles such as relatively uneconomical high usage times combined with a deficient charging infrastructure. Compared to cars with an ICE, PHEVs require a higher investment and can only become economically advantageous for high usage times. The investment cost amortize over the lifetime of a PHEVs, due to the lower operational cost. Considering the costs PHEVs are not expected to become cost effective by 2016 assuming a daily operation of less than 7.3 hours and an average speed of 40 km/h. However, by 2020 PHEVs the minimum operational time is expected to drop to 2.7 hours per day [4]. Apart for economic reasons customers are also hesitating because the charging infrastructure for EVs is not satisfactory. This is a problem because there is no economic incentive for companies to invest in charging infrastructure if only few people use EVs.

In order to take advantage of the benefits, overcome the hurdles mentioned, and raise public awareness, the German government launched several research projects that analyse the integration of several technologies in a smart grid. As a partner, the Reiner Lemoine Institute develops a simulation tool called SMINT (Simulation Model for Intelligent Energy Systems) for the energetic, economic, and ecological characterization of a micro smart grid. This new and universal tool accurately covers various present and future technologies by parameterizing key values and, at the same time, limiting computational time and complexity. The following research documents the component of SMINT that models electric mobility, specifically the charging infrastructure and the EV as one of the main elements of a micro-smart-grid.

A unique aspect of this analysis is the straight forward top-down approach which enables simulations of both controlled and uncontrolled charging in one tool. In addition instead of a control with a feedback loop that regulates the grid power, the behaviour of the control is

imitated by an open loop control. This allows sample times of up to one minute, low runtimes, and a high accuracy.

The power that is drawn from the grid can be controlled either by referencing the battery current or the grid power. In addition, also the boundaries of the SOC window are realized in two ways. The first algorithm measures the current into the battery, integrates it over time (coulomb counting), and limits it accordingly. The second one is realized by reducing the current, so that certain voltage limits are retained.

These developments are highly interesting for both research and industry. For research activities, the low computational requirements enable a variety of studies. Firstly, different energy management strategies that improve energy efficiency, battery lifetime, and energy availability can be tested. Secondly, it enables studies for the investigation of vehicle-to-grid (V2G), thermal preconditioning of vehicles, and an economic analysis and optimization. Thirdly, the dynamic behaviour of a large fleet of vehicles and their effect on the distribution grid can be studied and improved. For industry, this study incorporates essential parts that can be used for product and service innovation. Typical companies can be found in the field of vehicle fleet management, virtual power plant operation, and battery technology.

1.1. Structure of the Thesis

The charging infrastructure and the EV (including the charger and the battery technology) are modeled and simulated. The study is structured as follows: Chapter 2 gives an overview of the technology incorporated in the operation and the charging of an electric vehicle. Special focus is put on the battery because it is by far the most complex and important component. Chapter 3 introduces the framework for the representation of the charging infrastructure and the EV as a model. Here, the requirements and boundaries are set and basic modelling methodology and specifically different battery modelling approaches are presented.

Chapter 4 includes the implementation of the model and the open loop control strategy. Starting from the general structure this section outlines the way the submodels are constructed and programmed. In Chapter 5, the model and the control strategies are verified and a test case is presented. At the end, concluding remarks and an outlook on further work round up the thesis.

2. Electric Components

In this section, an overview of the relevant technologies that are necessary to transfer electric energy between the distribution grid and the vehicle battery is presented, along with their characteristics. In the following section, focus is placed on conductive charging, which represents the most common charging technique. Charging techniques such as battery exchange and inductive charging are not considered.

The aim of this section is to serve as a basis for modelling in terms of the following questions:

- Which technologies and components are used for charging and how do they interact?
- What are the effects that influence the performance of different components?
- How can the impact be quantified?

Starting from this point the devices that are needed for charging can be introduced. The most important are (a) the battery, (b) the battery charger (or power converter), (c) the cable connecting the car to the charging station, (d) the charging station itself, and (e) the cord connecting the charging station with the house connection box. Several fittings are necessary as well, such as (f) the cords inside the vehicle and the charging station and (g) the receptacles and the attachment plugs at the car and the charging station. All these components cause losses that can be either constant (e.g. standby) or vary with the power exchanged (e.g. ohmic losses). The standard IEC 62196-1 covers the interface between the charging equipment and the electric vehicle and specifies the mechanical, electrical, and performance requirements for involved plugs, socket outlets, vehicle connectors, and vehicle inlets [5].

For the representation of the major losses during charging, several German research projects showed the importance of the operation on the performance of a charging and discharging of an AEV. Sankey diagrams visualize the power flow and losses in [6] and [7].

2.1. Charging Station and Grid Connection

There are various different possibilities like battery exchange stations, high power charging stations (“shock charging”), and inductive charging for the provision of electric power. According to [8] in international standard IEC 61851 there are 4 different modes for conductive charging with the following characteristics:

- Mode 1 (AC): Charging using a standard plug max. 16A three phases without communication, charger is in the vehicle
- Mode 2 (AC): Charging using a standard plug max. 32A three phases, security and control functionality in cable or house
- Mode 3 (AC): Charging using a special plug max. 63A three phases, security and control functionality implemented in EV, charger is in the vehicle
- Mode 4 (DC): DC charging station with a special plug for EVs, the power equipment, security and control functionality is implemented in the charging station, the cable cannot be disconnected from the station

	Maximum power single phase	Maximum power three phase
Mode 1	3.7 kW	11.0 kW
Mode 2	3.7 kW	22.0 kW
Mode 3	3.7 kW	43.5 kW
Mode 4	DC-Low max. 38 kW	-
	DC-High max. 170 kW	

Table 1: Specifications of the maximum power demand according to industrial specifications [9]

The charging station is the device that connects the car to the power grid. It also sends the control pilot signal to the charger for starting the charging process and disconnects the EV in case of a fault. For a power analysis it is important to research the efficiencies across the power flow chain. For the charging station the major losses originate from:

- the current limitation, the 12V pilot for the contacting process, and standby (~10W) [7];
- and eventually additionally switches, internal cables, the screen, and the master control station [9].

For the cable losses, standard equations for AC and DC power systems can be used. In AC systems the power flow is determined by the equation:

$$P_{3\phi} = 3 \cdot P_{1\phi} = 3 \cdot V_{pn} \cdot I_{AC} \cdot \cos(\varphi) \quad (1)$$

where $P_{3\phi}$ is the transmitted power for 3 phases respectively, $P_{1\phi}$ for one phase, V_{pn} the root-mean-square (RMS) voltage from phase to neutral, I the RMS current, and $\cos(\varphi)$ the power factor. In a DC system, the power flow is calculated by:

$$P_{DC} = V_{DC} \cdot I_{DC} \quad (2)$$

Where P_{DC} is the power transmitted V is the voltage and I the current. The losses for AC and DC are

$$P_{l,3\phi} = 3 \cdot I_{AC}^2 \cdot R_{cable} \quad (3)$$

$$P_{l,1\phi} = I_{AC}^2 \cdot R_{cable} \quad (4)$$

$$P_{l,DC} = I_{DC}^2 \cdot R_{cable} \quad (5)$$

with

$$R_{cable} = \frac{\rho \cdot l}{A} \quad (6)$$

where $P_{l,3\phi}$ and $P_{l,1\phi}$ are the losses for three phases and one phase, R_{cable} is the cable resistance, ρ is the specific resistance, A the diameter of a cable, and l the length. In DC systems the length has to be multiplied by two, in order to consider both the high and low voltage cables.

For the design of the connection from the house connection box to the electric appliance, the German standard DIN 18015 can be consulted. It states that the allowed voltage drop depends on the required apparent power and the distance of the house connection box to the receptacles [10]. The charging cable is typically made out of copper, 5 meters long, and has a cross section of 10 mm^2 [9]. According to [7] the resistance is $2 \cdot 0.2 \text{ m}\Omega$ for the plugs and $2 \cdot 21.7 \text{ m}\Omega$ for the cable. This amounts to losses of about 11 W for a one phase charging system when charging with 3.68 kW.

2.2. Battery

A battery is a storage device consisting of one or more electrochemical cells that convert the stored chemical energy into electricity. The most prevalent battery technologies that are used in the automotive sector today are lead acid batteries. In conventional cars these batteries are used to provide the starter motor, the lights, and the ignition system with power. Because of their low specific weight and volume, Li-ion batteries are the most promising technology for traction [2]. Hence, they will be the only battery technology considered. Accordingly, the usage of the term battery implies Li-ion batteries in the course of the thesis.

The most important value when characterizing a battery is the capacity, which is measured in ampere hours (Ah). For the operation the current state of charge (SOC) of the battery is essential. It is represented as a percentage and defined as follows:

$$SOC(t) = \frac{\int I_{bat}(t) \cdot dt}{Q_{nom}} = \frac{Q_{act}}{Q_{nom}} \quad (7)$$

where I_{bat} is the current to the battery, Q_{act} is the actual capacity stored in the battery, and Q_{nom} is the nominal capacity of the battery. The DOD is defined as:

$$DOD(t) = \frac{Q_{nom} - Q_{act}(t)}{Q_{nom}} = 1 - SOC(t) \quad (8)$$

For small time steps Δt the SOC is approximated as:

$$SOC(t) = SOC_{(t-1)} + I_{bat} \cdot \Delta t \quad (9)$$

and when just considering the SOC window the SOC becomes:

$$SOC_{window} = \frac{Q_{stored} - Q_{min}}{Q_{max} - Q_{min}} \quad (10)$$

This makes an analysis easier because the offset of the minimum and maximum capacity, Q_{min} and Q_{max} , is not incorporated. The consequence is that the value varies are between 0 and 1.

2.2.1. Performance Indicators

From a user perspective, the battery performance in relation to an EV is energy capacity, efficiency, and life expectancy. These parameters are strongly dependent on a number of variables such as temperature, depth of discharge (DOD), charge and discharge rates (CR), and the number of cycles (CN).

The lifetime of a battery is defined as the time between startup and the outage of a battery. According to German standard DIN 43539 / part 4 and also internationally [11], outage is reached as soon as the capacity drops under 80% of the rated capacity. Similarly, there is a definition that represents the state of health (SOH) of a battery. It is defined as:

$$SOH = \frac{Q_{aged}}{Q_{nom}} \quad (11)$$

where Q_{aged} is the reduced maximum capacity due to aging and Q_{nom} is the nominal capacity at the beginning of the lifetime. A mathematical approximation of the capacity fade can be found in [12].

The charging efficiency according to [13] is defined as:

$$charging\ efficiency = \frac{\Delta Q_{in}}{\Delta Q_{out}} \quad (12)$$

and the energy efficiency as:

$$energy\ efficiency = \frac{\Delta E_{in}}{\Delta E_{out}} \quad (13)$$

where ΔQ_{in} is the amount of charge during charging, ΔQ_{out} the capacity that is discharged during one cycle, and ΔE_{in} is the electric energy during charging, and ΔE_{out} the electric energy during discharge. According to [13] for temperatures higher than the freezing point the energy efficiency is above 95%. The energy efficiency for $T=-20^{\circ}\text{C}$ drops to 88%.

In general, it is possible to distinguish between short term effects and long term effects, as well as reversible and irreversible effects. Short term is defined as having a significant effect (change in thévenin voltage or resistance of about 1%) during one cycle whereas long term effects have a consequence after several cycles. Usually the car operation is optimized in order to avoid harmful conditions. However, they cannot be fully avoided due to operational requirements. In some cases there must be a trade-off due to a condition having both positive and negative effects. For example, higher temperatures reduce the internal resistance, but at the same time accelerates aging.

	Long term	Short term
Irreversible effects	NC, temperature, CR, DOD and calendary time on impedance	-
Reversible effects	Self-discharge on capacity	Temperature and CR on open circuit voltage Temperature and SOC on impedance

Table 2: Effects of external and operational parameter on entities of the electric circuit model

The conditions in Table 2 are not reflected in specification sheets in which the data is generally idealized and set to specific parameters. However, this is only natural considering the complexity of this electrochemical device. Likewise the information provided in scientific papers is also limited due to the necessity of large amounts of data. Table 3 summarizes the effects that influence the performance of a battery and compares their weighted impact. The effects are explained in the following chapters in detail.

	Energy efficiency during a cycle	Energy efficiency long term	Energy capacity reversible / short term	Energy capacity irreversible / long term
Temperature	low	medium	high	medium (avoidable)
Charge or discharge rate	medium	medium	medium	medium (avoidance limited)
Discharge to low DODs	very low	medium	No	medium (avoidable)
Number of cycles	No	medium	No	medium
Calendary time	very low	low	very low (self-discharge)	No information found

Table 3: Overview of the influence of operational conditions on the performance of EV-batteries

Figure 1 shows the self-discharge of a battery for the duration of one year. It shows that the capacity drop is less than 1 % per day or 1 mV for a battery cell with a nominal voltage of 3.7 V. Considering that an EV is used several times a day in order to account for the higher investment cost this effect can be neglected. As such, this effect is not investigated further. However, it would not be problematic to include it in a model.

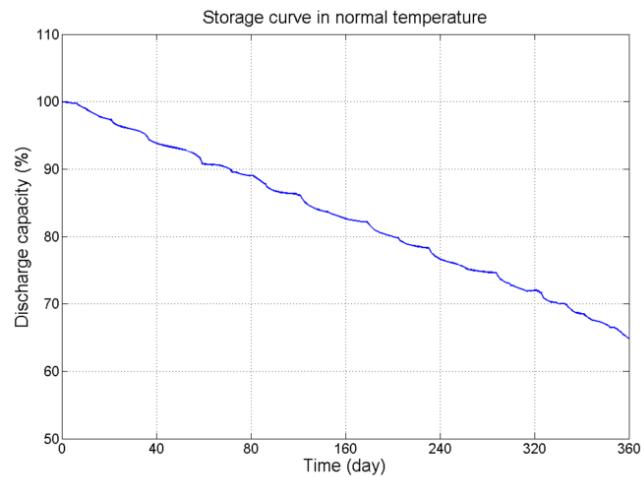


Figure 1: Self-discharge of a battery over a year [14]

A battery simulation at the Danish Technical University [14] has shown that the performance of the battery depends heavily on the operational conditions. For different use cases the battery lifetime varies between 14 and 27 years and the efficiency between 90.8 % and 95.5 %. High lifetime is expected for slow charging and work home driving profiles, while reduced lifetimes are expected for a large number of cycles and higher usage times. The following chapters describe the complex relationship between the performance and the operational conditions such as temperature, DOD, CR, and the number of cycles.

2.2.2. Temperature and Number of Cycles

For a detailed analysis of the Li-ion technology the battery of the Boston Power company was investigated using the datasheet [15]. The results are summarized in Table 4 and Table 5. The data for five different discharging curves were extracted using eleven to 18 data points and interpolated as well as extrapolated using a cubic spline function. When comparing the extracted data with given data (nominal energy capacity, nominal capacity) in the datasheet the results are satisfying, with a variation of less than 1%.

The results show that high temperatures increase the capability of the battery to store energy. For example, at a temperature of 45°C the capacity is 3.7% higher than if the battery were at 25°C. This is similar to the results of [15] and unique when comparing with other battery technologies [13]. For temperatures above 45°C, the capacity decreases. Taking 25°C as a base case, both the capacity and the energy rise towards higher temperatures. However, when considering the energy the effect is even stronger. The energy available at -40°C more than halves and the capacity drops to 58%. When solely looking at the capacity, a misinterpretation of the effect of high discharge rates is most likely. Therefore the focus should be on the energy which accounts for lower operating voltages.

Conditions	Parameter variation	Energy available	Capacity available
Discharge rate: 0.5C Discharge Voltage: 2,75V	45°C	19.5 Wh	5.4 Ah
	25°C	18.8 Wh	5.2 Ah
	0°C	16.2 Wh	4.6 Ah
	-20°C	13.3 Wh	4.0 Ah
	-40°C	8.9 Wh	3.0 Ah

Table 4: Energy available for discharging batteries at different temperatures based on datasheet [15]

According to [13] the behaviour is ideal for a wide range of variables with the charging efficiency exceeding 99%. Exceptions are SOC's higher than 95% and temperatures underneath the freezing point (Figure 2). The energy efficiency of a Li-ion battery is also high (~ 95 %) for a wide range of conditions as compared to other technologies.

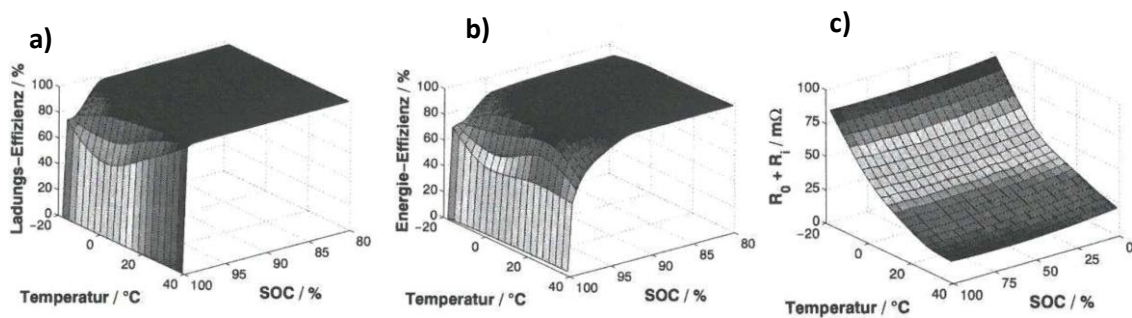


Figure 2: a) charging efficiency, b) energy efficiency and c) resistance (vertical axis) depending on the temperature (bottom left axis) and the SOC (bottom right axis) [13]

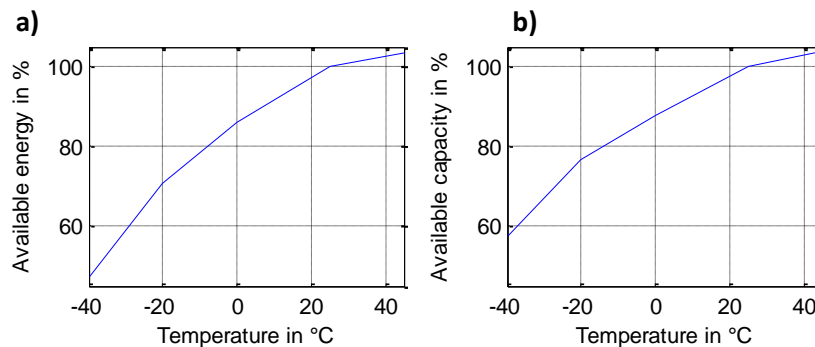


Figure 3: Influence of temperature on a) available energy and b) capacity based on [15]

Nevertheless, it is not recommended to operate at high temperatures due to faster aging. According to [11] using the battery at 45-50°C can halve the lifetime. Furthermore the ohmic resistance increases over time while the polarization resistance stays almost constant. At 40° C the ohmic part increases about 20% for hundred cycles (1C charging and discharging current and 100% DOD variation). These are rather detrimental conditions. However, the conclusion to be drawn is that the electric performance degrades over time. [16]

2.2.3. Depth of Discharge and Number of Cycles

In general operating the battery at high DODs is harmful and significantly decreases the lifetime (Figure 4). According to [15] discharging a battery up to 100% instead of 90% of DOD could result in about 1000 cycles of difference in lifetime. The lifetime decreases to more than 3000 cycles for DODs less than 80%. So to preserve the battery lifetime, the DOD level should not exceed the 80% for pure EVs and 60% for PHEVs. [11] Assuming a utilization ratio of about 500 cycles a year (DOD is 80%) the average lifetime of a HEV-battery is 4 years and for PHEV (DOD is 60%) it is 6 years. Concluding from Figure 4 the correlation between life expectancy and the operation is shown. For a DOD of 10 % energy is exchanged 40000 times during the lifetime and falls to 2000 times for rates of 80%.

Similarly to the effect in temperature also for high DODs the internal resistance increases over time. That has a negative effect on the electric performance. To show the effect a test is performed in [16] for 150 cycles at a temperature of 40°C and CR rates of 1C. Quantitatively it can be mentioned that for 60 % DOD the internal resistance rises to 150% of its initial value while the rise is only 130% for 20% DOD.

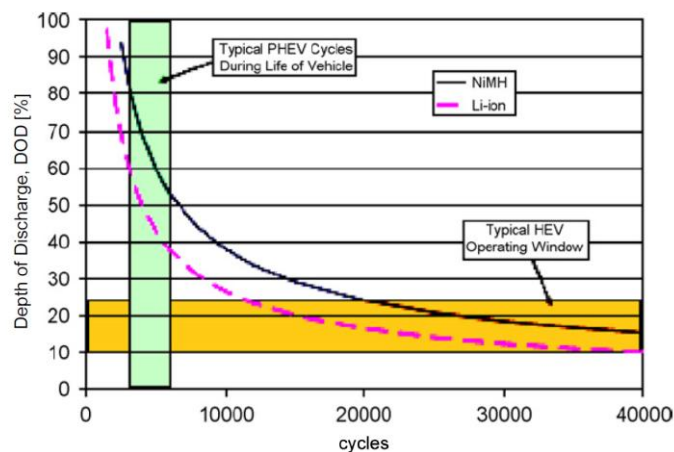


Figure 4: Life expectancy for different DOD rates [17]

2.2.4. Charge Discharge Current Rates and Number of Cycles

The influence of charge and discharge rates on the battery capacity, also known as Peukert-effect, describes the decrease in capacity at high current rates (CRs). The effect is studied based on datasheet information [15] and the results are summarized in Table 5. The trend shows that for high CRs the Peukert effect is moderate and that the available capacity even increases (Table 5). The reason for this can be a temperature increase of the battery. When looking at the energy instead of the capacity the effect is clear. The energy available decreases for higher discharge current rates from 19.4 Wh (0.2 C) to 18.3 Wh (2 C). This has two reasons: One is that, due to the Peukert effect the capacity is reduced, the other is that the average voltage is lower.

So, from an energetic point of view it is advisable to operate at low CRs. But in reality, the occurrence of high discharge rates is not avoidable, e.g. during the acceleration of a vehicle. Also low current rates extend the charging time, which is user unfriendly.

In the long term charging and discharging the battery at high discharge rates harms the battery. As an example charging at 2 C instead of 1 C or C/2 can halve the lifetime [11]. Also high CR rates cause a rise in the ohmic part of the internal resistance which negatively affects the electric performance (energy efficiency, energy capacity) [16].

Conditions	Parameter variation	Energy available in Wh	Capacity available in Ah
Temperature=23±2°C Discharge voltage lower limit: 2,75V	0.2 C or 1.1 A	19.4	5.3
	0.5 C or 2.7 A	18.8	5.2
	1.0 C or 5.3 A	18.5	5.2
	1.5 C or 8.0 A	18.4	5.2
	2.0 C or 10.6 A	18.3	5.28

Table 5: Energy available during discharging at different CRs based on datasheet [15]

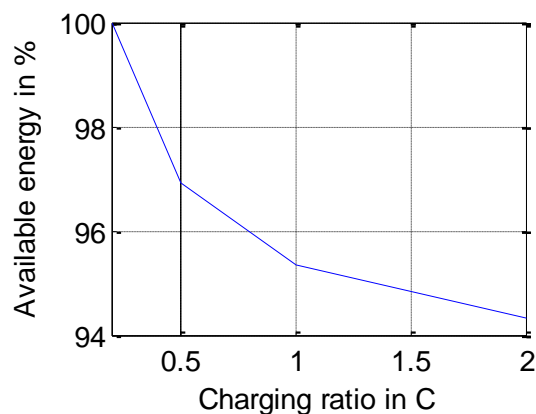


Figure 5: Influence of CR on available energy based on [15]

2.3. Auxiliaries in Cars

When comparing AEVs with conventional cars, there are several auxiliaries that are necessary in both kinds of vehicle, others are technology specific. A summary of different auxiliaries including maximum power and average power requirements for EVs is listed in [18]. The average power is stated to be 2.47 kW. However, the demand of the auxiliaries heavily depends on the energy management of a car, the driver behaviour, and the external conditions.

In cold climates the electricity consumed by the high voltage heater reduces significantly the available capacity of the battery for driving. In electric cars for very low temperatures of -15°C heating amounts to up to 4.5 kW and can be reduced to 3 kW if air from the interior is mixed with fresh air [19]. Additionally pumps, fans and other equipment connected to the high and low voltage network add up to the power demand of EVs. Other typical auxiliaries used in both conventional cars and EVs that have a high electricity demand are vacuum pumps for braking enhancement and high voltage compressor for air conditioning [4].

Compared to this the power required for the charging interface module that enables the communication with the charging station and activation of the charging process is rather low (4 W).

A very important auxiliary in terms of energy efficiency is the battery charger which can be categorized into off-board and on-board types with unidirectional or bidirectional power flow. Unidirectional charging reduces hardware requirements and simplifies interconnection issues. Bidirectional charging supports battery energy injection back to the grid but increases complexity [20]. The performance of the charger depends on the technology. Chargers that allow a wide range of input voltages are applicable worldwide (e.g. Europe ~235 Volt and USA / Japan ~115 Volt) but generally have a lower efficiency. Chargers that are optimized for a certain input voltage range perform better.

In literature various values for the efficiency can be found. In [7] a charger efficiency of 93% was assumed which is in-line with information from the industry (up to 94%). A rather good efficiency was measured in [21] with efficiencies ranging from 95.5 % for full load to almost 98.5 % for a load of 1.5 kW (Figure 6). The efficiency curve characterizes a bidirectional on-board charger. In [22] a charger efficiency of 88 % was measured and then used for simulations.

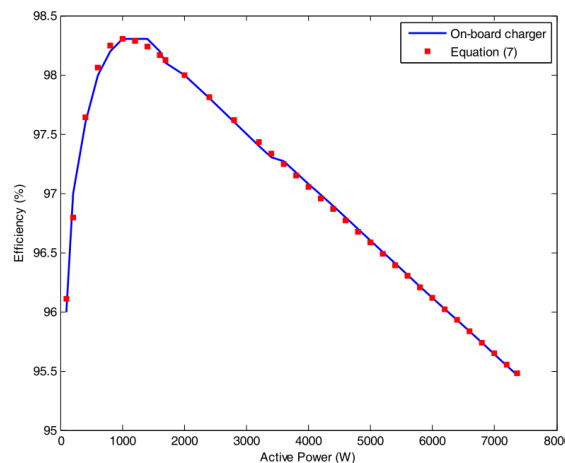


Figure 6: Bi-directional charger performance

3. Modelling Approach

In order to clarify the major implications, the following sections summarize and define the terminology which is necessary to describe complex energy systems. Furthermore, the general requirements of the model are established and boundaries are set. This will ensure that the work achieves the goals and can be used in the defined application.

3.1. Simulation Requirements and Validity

The purpose of the model is to estimate the performance of different configurations, components and designs as well as to mirror the impact of internal as well as external operational conditions. Consequently, the requirements and constraints can be defined as follows:

- High precision and validity
- Simplicity of the characterization
 - Based on datasheet and generic information
 - No special measurements or data obtained by impedance spectroscopy for battery parameterisation
- Low simulation time
- Validity for fixed sample times in the range of 1 minute or less and simulation periods of up to 1 year

This will permit testing different energy management strategies that improve energy efficiency, battery lifetime and energy availability, enable optimized engineering designs and allow simulating various different parameterized models for the investigation of a fleet of electric vehicles.

Required functionalities of the model:

- Consideration of regenerative braking and V2G in simulation
- Uncontrolled charging as well as controlled charging with variable charging power
- Model applicable for all electric vehicle drivetrains with typical examples being Citroen C-Zero, Mitsubishi i-Miev, Peugeot iOn and Smart electric drive
- Different charging modes according to IEC 61851
- Considerations of CR on battery performance
- Only conductive charging

The major limitations related to the model are defined as:

- Modelling of a specific charging station and a specific car not modelling of the behaviour of a fleet of cars
- European or international standards as a basis for technical applications
- Use of Matlab Simulink for the implementation and compatibility with other models that consume, produce or store electricity
- No modelling of battery exchange and inductive charging

Considering the requirements there are opposing objectives. The reason for this is that as a rule of thumb a more complex model gives more accurate and exact results, but requires higher computational capacity and more knowledge about the components involved. As a result, a trade-off between precision and complexity is ideal that supports the required functionality and is capable of describing the major variables involved.

3.2. Modelling Basics

The general approach for modelling the charging infrastructure and the electric vehicle is to first apply system thinking to understand relationships and linkages between the components that form the system. Here, it is essential to understand that a system can only be defined by the function and not by the components it comprises. In modelling complex systems the general methodology is the following: First, the system is divided into smaller subsystems according to their function. These are described by independent models. By combining the different submodels and defining their interactions the behaviour of the entire system is accomplished. [13]

The step from the subsystem to the submodel can be accomplished in two different ways. One is called physical and the other phenomenological modelling. In physical modelling electrical, chemical, or thermodynamic equations are used for the characterization, which can be a rather complex task when modelling e.g. the interaction of molecules in an electrochemical device.

For reasons of simplification and if the physical conditions and correlations are not known, a system or its entities can be described phenomenologically. This means that the entity is treated as a black box and only the correlations between input and output parameters are analysed. However, in that case the detailed processes are not known so there is danger of not considering all possible effects. This makes a thorough verification of the characteristics necessary which is in general more complex than in physical modelling. Also, great care has to be put on the separation of the underlying effects and relations. [13]

Today, in many existing applications hybrid modelling is used, which combines phenomenological and physical models. The chosen approach is one factor that determines the complexity and the accuracy of the model.

Concluding a model is a description of the relations of a certain physical situation. The relationships are described using mathematical expressions or correlations whereas the quantities appearing in the equations are interpreted either as variables, parameters, or constants. Variables in that sense are not known and have to be calculated, while parameters can be determined and are therefore predefined. Constants in that sense are parameters that are determined by nature or have a permanent and immutable character. Also, a distinction can be made between time variant and time invariant parameters.

A simulation is representing a physical situation or a process over time, whereas the basis for the simulation is a model. If a system is either „warming up" or taking its time to respond to a disturbance, transient behaviour occurs. It is able to describe the transition between different

states. Whereas, if a system for an interval of time has properties that are not changing the system is in steady state. The derivative of state variables over time is zero.

In order to achieve a certain engineering decision, certain tools are developed with this work representing one of them. These tools can be used to fit to a certain application by varying certain parameters and examining the effect on the results. This makes testing of different components possible, without changing the underlying relations. Especially when analysing various use cases and researching different configurations, the comparability and adoption becomes a powerful characteristic of a parameterized model.

3.3. Battery Models

Therefore, an optimal representation of the efficiency, the capacity and the state of health of a battery is crucial. This chapter is supposed to establish the basic advantages and disadvantages in terms of accuracy, computational complexity, configuration effort, and analytical insight of different models discussed in literature. Similarly to the general modelling approaches presented in the previous Chapter 3.2, also for batteries there are three approaches. It is not intended to describe specific models. Examples are listed in [14] and [23]. Rather a categorization and review of the categories is presented. Based on this a decision can be achieved which approach is suited best for the application in the tool.

3.3.1. Physical or Electrochemical Models

This method is based on the internal workings of the battery. Thus, the physics of the battery is included in electrochemical models, making them very demanding calculations with regard to time and computation power. Electrochemical models are typically used to optimize the battery design and the composition. Hence, this approach is not considered as a possible solution, as the focus remains on the battery performance estimation, rather than the physical design. Also these models are known to require high computational power, which makes them inappropriate for a series of simulations in connection with other green technologies. [14]

3.3.2. Empirical or Phenomenological Models

This approach is simple when there is only one effect to be considered and the operation is invariant. This would be the case if the car is charged and discharged at the same temperature to the same DOD. Also in that case this approach needs a low amount of data and has low computational requirements. However, in this thesis dynamic simulations are required with changing conditions of the environment and the operations. So this approach seems to be inappropriate, due to low accuracy of the results or high amount of measured data needed.

3.3.3. Electric Circuit Models

These models are based on the representation of the battery by an electrical circuit. What is different to empirical models is that measurements and other data are the basis for parameterizing values of the electric circuit. Typically a voltage source is connected in series with resistances, RC circuits and inductances modelling the voltage response of the battery.

The complexity depends on the dynamics that are supposed to be reflected. The elements of the electrical circuit change over time which is analysed in Chapter 2. Generally these models can be categorized in abstract approach and mixed approach [13]. Abstract models consist solely of an electric circuit, whereas mixed models are extended by a thermal (mostly physical) model or ageing models (mostly empirical). Using these models it is possible to take different effects and transients into account, by adding and adjusting the values of the electric circuit elements [24]. E.g. in [13] the OCV adjusts according to the CR rate, the SOC, and the temperature. The inner resistances, capacitances and inductances vary according to the temperature and the SOC. Equivalent circuit models are seen as an intermediate approach between electrochemical and physical models, where the model accuracy and computational efficiency are balanced [24].

One big issue when dealing with equivalent circuit models is parameterization. For complex models impedance spectroscopy combined with a mathematical fit is used to define the elements of the circuit at different conditions. For determining the OCV though a simple and common approach is presented in [14].

A typical method based on battery data sheets is presented in Trembley et al. [25]. This battery model is also included in the Matlab/Simulink library SimPowerSystems and has the following advantages and disadvantages:

Advantages	Disadvantages
represent the transient state of the battery cell	limited to describing the charge and discharge curves of a battery cell at constant temperature and aging
simple parameterization	level of accuracy is unknown and will be very dependent on the available operation information from the manufacturer
	accuracy cannot be improved
	internal structure of the model is not known

Table 6: Disadvantages and advantages of the model of Trembley et al. [25]

Also the approach in [24] is based on data sheet information, but considers the temperature as well as the discharge rate. Another difference is that there is a differentiation made between the internal charging and discharging resistance. The idea is to fit the OCV and the resistances, so that the resulting voltage behaviour matches with the datasheet information.

Nevertheless the problem remains that the information provided by the manufacturer is generally idealized and does not capture the complexity of the electrochemistry. The internal resistance R_i provided in the datasheet is measured at low currents and is about 50% to 100% higher in reality [26]. However, in this application abstract equivalent circuit models based on datasheet information are the best option. They do not require measurements or complex physical modelling.

4. Simulation of Charging and Discharging Process

Considering the requirements and basic modelling considerations outlined in Chapter 3 and the technology presented in Chapter 2, a model was developed. It is a top-down approach with the energy management system controlling the power of the EV (controlled charging). Also uncontrolled charging is possible. In that case e.g. the power is set to the maximum power supported by the hardware according to the charging mode and the capacity of the charger. Furthermore the functionality of investigating V2G is possible. V2G is not a standard in real applications but offers great potential in terms of provision of grid services.

The top-level layout is shown in Figure 7. The reference input for the electric vehicle model is the grid power. The output is the actual power and the SOC. In the case of uncontrolled charging the electric vehicle is not an integrated part of the energy management system and stands as its own. Simply the outputs like SOC and power demand can be measured.

The parameters determining the behaviour of the electric vehicles can be divided into two categories:

1. The operational parameters are composed by time variant values for the vehicle speed, the auxiliary power demand, and the information if the EV is connected or not.
2. The design parameters are time invariant and represent the majority of the total number of parameters. Here typical examples are connected to the EV (e.g. battery parameters) and the charging infrastructure (e.g. cable parameters).

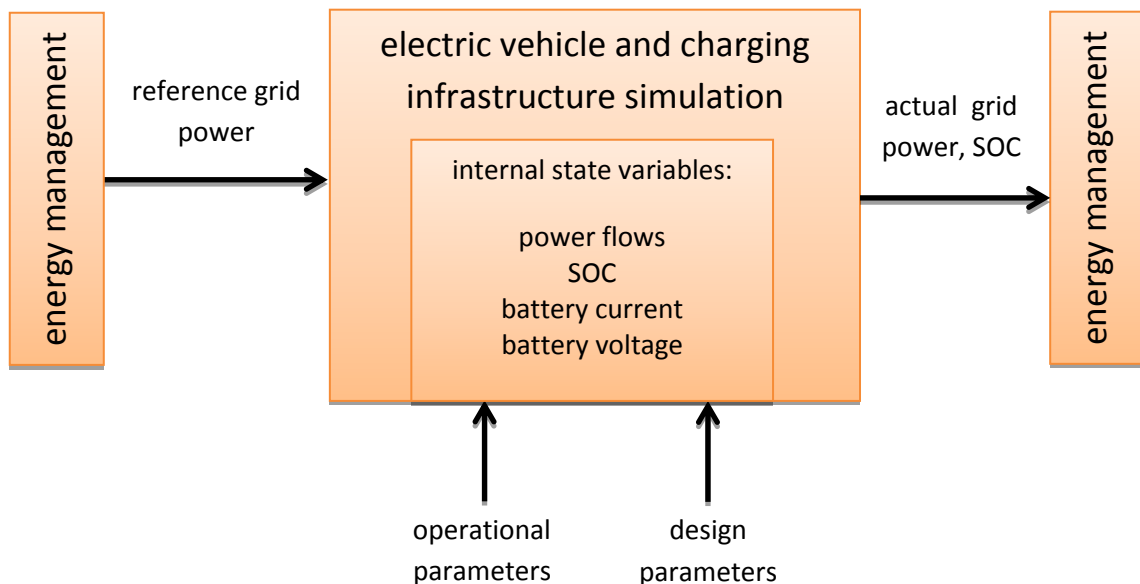


Figure 7: Layout of the model for controlled charging of the electric vehicle

Modelling the auxiliaries is outside of the scope of this work, because it is not directly connected to the charging process. However, the influence and the power can be set by a time variant parameter. This vector should match up the power demand of the auxiliaries (e.g.

preconditioning) with the itinerary. For more information on which auxiliaries exist and their power demand, please consult Chapter 2.3.

4.1. Internal Structure

Due to fixed sample times of 1 minute the reaction of the control has to be immediate. This makes a control with feedback loops inappropriate. Also, iterations are not an option due to limited computational times. Therefore, the only option is an open loop control system which can set the desired state directly.

The layout of the simulation tool that is controlled by the reference input of the energy management system is visualized in Figure 8. First, the reference grid power at the house connection box is converted into the equivalent power at the OSS, considering transmission losses and the efficiency of the power electronics. This feeds in a model of the battery which determines the reference battery current. For constant current operation the model simplifies because the algorithm that calculates the equivalent current for a certain power is not necessary.

Except of that the procedure is the same and continues with two options that control the upper SOC level. One is based on Coulomb counting and the other on a maximum voltage. Both approaches are presented in more detail in Chapter 4.3.2. So, in total there are four different control options which are a combination of different settings for the reference input (battery current or grid power) and the charging limitation (based on Coulomb counting or voltage). The algorithm continues with calculating the SOC and the actual battery power. Then the power that is provided by the battery is dispatched to the grid, the auxiliaries and the electrical machine according to the reference power and the reference car power at the OSS. At the end, the grid power is converted back from the OSS to the equivalent power at the house connection box.

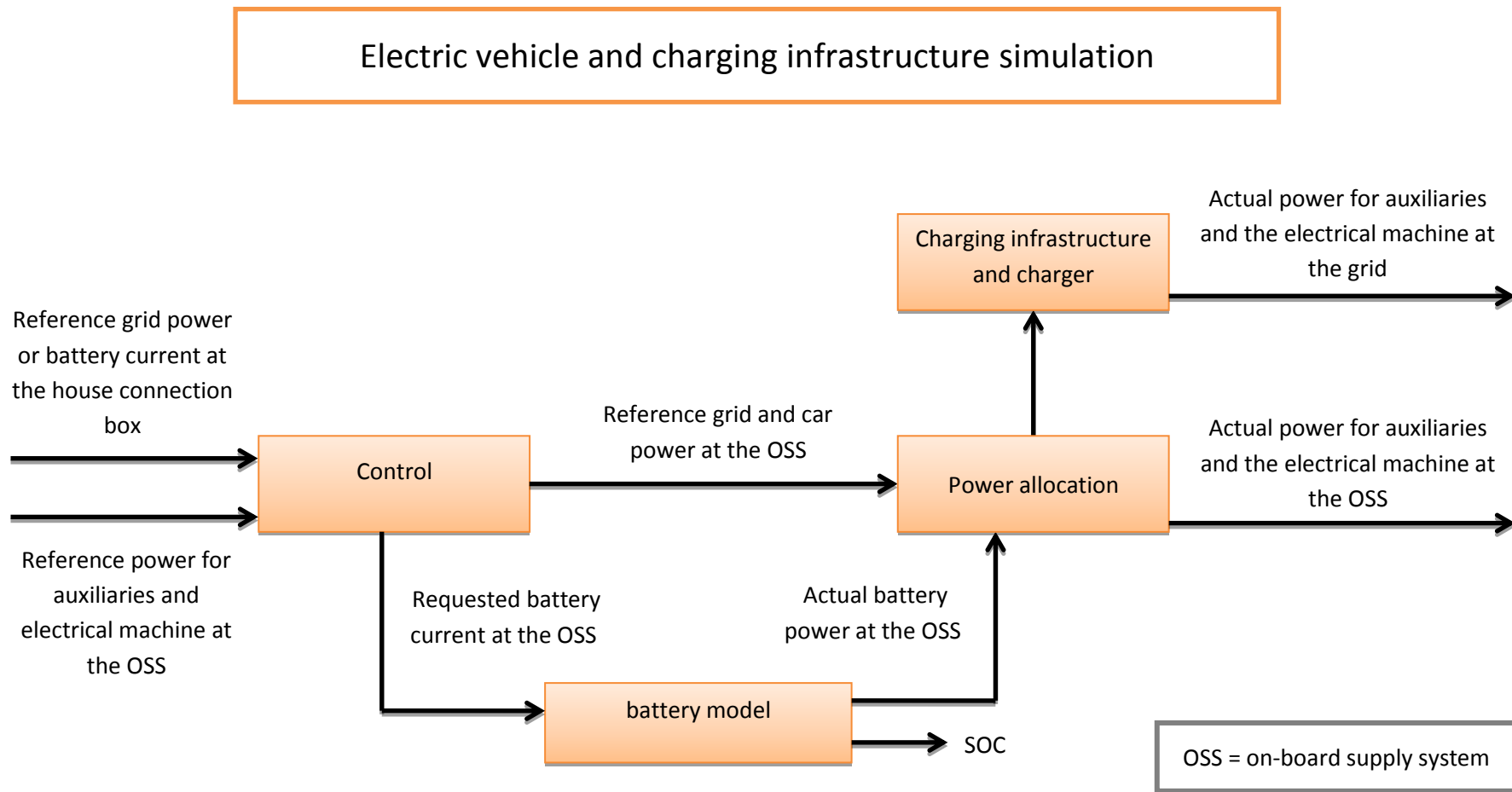


Figure 8: The flowchart of the electric vehicle and charging infrastructure model

4.2. Charging Infrastructure and Charger

The charging infrastructure and the charger are involved in two parts of the model. In the first part the reference grid power is transformed to an equivalent requested power at the OSS. In the second part the actual power of the grid is transferred from the OSS to the equivalent at the house connection box.

Both power losses and hardware limitations are taken into account in the simulation. The losses considered for the charging infrastructure are only the cable losses because they can represent major losses under certain conditions. Other losses caused by switches, cords and communication are not considered because they are less than 1 % (Chapter 2.1). The cable losses calculation is based on Chapter 2.1 and the result between single phase and 3 phase transmission can be compared in Figure 9 a) and b) assuming a copper cable with a cross section of 10 mm², a cable length of 20 meter and a $\cos(\phi)$ of 1. In a single phase system the losses are up to 0.5 % for a transmission of 3.7 kW and in a three phase system up to 1% for 43.5 kW. This value is rather low; but may rise for a higher resistance.

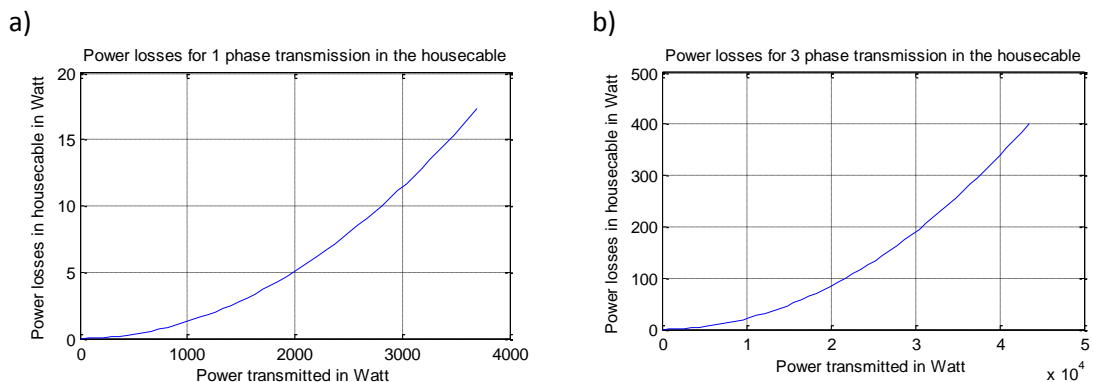


Figure 9: Transmission losses for single phase and three phase transmission

For the charger the efficiency curve presented in Chapter 2.3 based on [21] was implemented. The curve is normalized to the rated capacity of 8000 W and assumed to have the same characteristic, when operating both as a rectifier or an inverter (Figure 10). The efficiency can be adjusted according to the application and the charging technology by importing different curves and the rated capacity. Also the characteristic of a DC off-board charger can be implemented in this way.

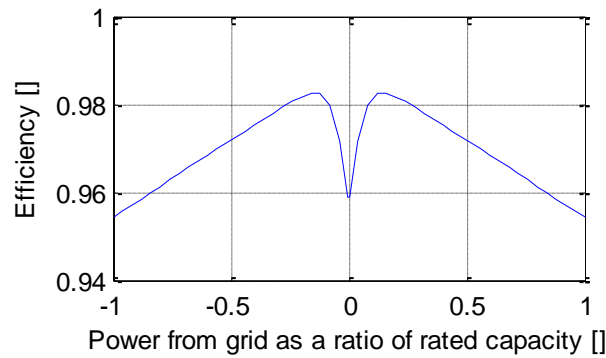


Figure 10: The performance of the bi-directional converter

Other effects apart from part load behaviour were not considered. The reducing effect of frost on the charger performance was not considered. Saturation blocks in Simulink limit the requested power according to hardware boundaries (charging mode and capacity of the charger). That way both controlled charging and uncontrolled charging can be simulated with the same model structure. By setting the reference grid power to infinity will automatically be reduced to the maximum possible values.

4.3. Electric Vehicle Battery Simulation

Different approaches for battery modeling are presented in Chapter 3.3. The conclusion of this chapter is that the only suitable approach is equivalent circuit modelling. The model implemented is a constant resistance in series with a SOC dependent open circuit voltage (Figure 11). This model does not include any resistances in parallel with a capacitance and is therefore limited to quasi-steady state considerations. The advantage is the simplicity which results in low parameterization and coding effort, as well as low runtime.

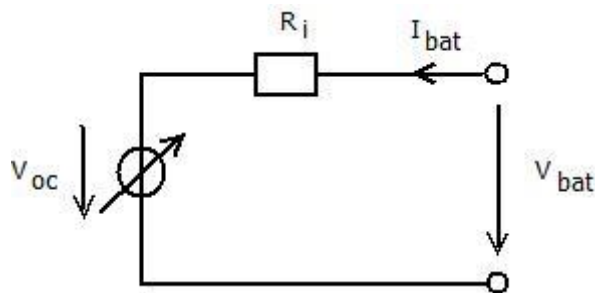


Figure 11: Equivalent circuit model of battery cell

4.3.1. Assumptions

The assumptions for the battery model are the following:

- The internal resistance is supposed to be constant during the charge and discharge cycles and does not vary with the amplitude of the current.
- The model's open circuit voltage is the average between the discharge and the charging curve for 0.7C.

- The capacity of the battery does not change with the amplitude of the current (No Peukert effect). However the voltage does change.
- The effect of the temperature of the battery is not considered.
- The self-discharge of the battery is not represented.
- Every cell has the same characteristic, the same parameters and the same behaviour; there is no mismatch.
- The charging efficiency is not considered.
- Aging is not considered.

The temperature dependence was not considered due to the following reasons: From available data no correlation between the battery temperature and the resistance or OCV can be developed because the datasheet information is based on the ambient temperature. Furthermore the effect of temperature on the terminal voltage is presented. Furthermore it cannot be distinguished between effect of temperature on resistance or OCV. Also it is not considered concerning the maximum capacity that can be charged.

The open circuit voltage can be approximated as the average between the charging and discharging curve in the SOC window in the linear zone.

$$V_{OC}(SOC) = (V_{charge,0.7C}(SOC) + V_{discharge,0.7C}(SOC))/2 \quad (14)$$

For low and high SOC this assumption does not hold (Figure 12). However EVs are usually operated in the linear zone between ~90 and 15 % [24], so the average voltage is a good estimate for the OCV. The fact that the OCV increases during longer periods of charging and decreases for discharging as described in [13] is not considered. The resistance was assumed to be the average resistance for an SOC between 20% and 80%. Considering it constant simplifies the simulation and does cause insignificant changes in the resulting terminal voltage.

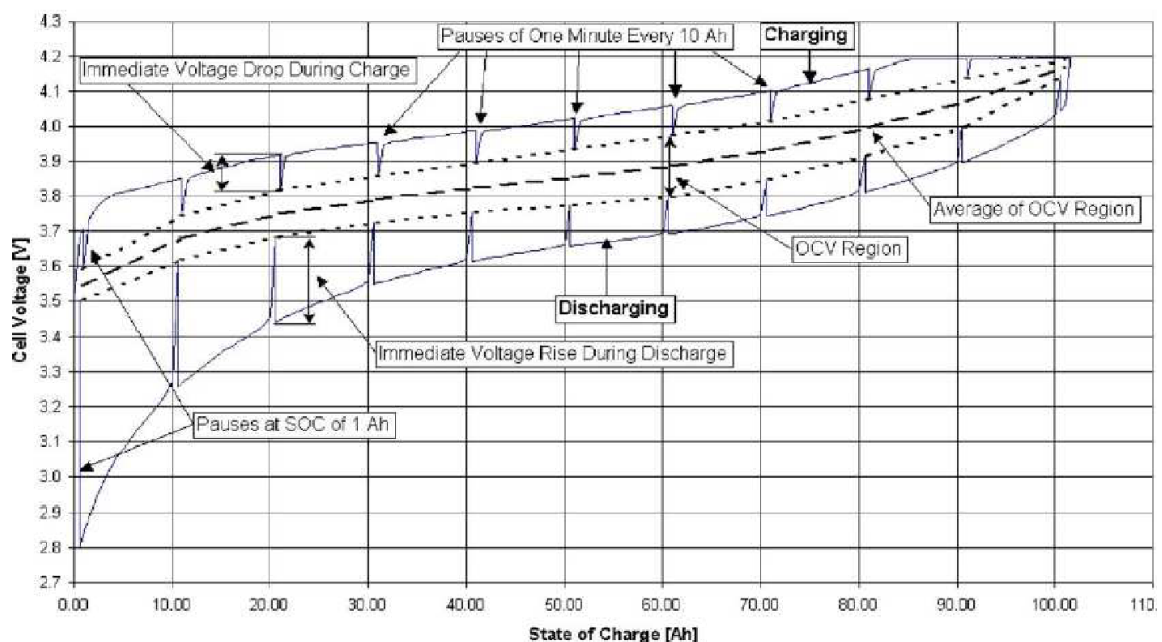


Figure 12: Graphical explanation of determining the open circuit voltage from a charge and discharge curve [15]

Furthermore, analyses of a datasheet have shown that the Peukert effect has very little effect on the capacity (Chapter 2.2.4) and even increases for high discharge currents. Therefore it can be neglected. The self-discharge of the battery is neglected due to the low influence (Chapter 2.2.1). The assumption that every cell has the same behavior is motivated by the fact that the model is supposed to represent the average performance of a cell, although in reality cells even from the same kind vary significantly in their characteristics [16].

The cells are interconnected to modules so that the energy capacity can be scaled. In Chapter 2.2.2 it is presented that the charging efficiency of a Li-ion battery is almost ideal and can be considered to be 100%. Nevertheless together with the self-discharge this assumption can cause problems in the long term due to Coulomb counting. For long time periods this will result in diverging of the model with the reality. Aging is not considered in the sense that the parameters do not change automatically. Nonetheless, changes in the parameters can be incorporated by either decreasing the capacity or by varying the electric parameters of the model (mainly the ohmic resistance).

4.3.2. Implementation of the Control

The open loop control of the battery is implemented as two stages. The first stage determines the charge and discharge rate while the second stage limits the current, so that the SOC window is maintained. For both stages there are two control options.

In stage one Option a) the input is the reference grid and car power including auxiliaries and the electrical machine. For determining the CR the internal states of the battery are essential. Basically the algorithm implemented solves the equivalent circuit by taking into account the open circuit voltage, the reference power and the resistance (Figure 13). The methodology is presented in Chapter 4.3.3. Option b) is a simplification because the CR is set directly as the reference input for the second stage. An algorithm is therefore not necessary.

The second stage sets the boundaries for the SOC window by reducing the battery current (Figure 14). In option a) the current is limited so that the SOC remains inside the operational window (Coulomb control):

$$Q_{min} < Q_{actual} + I \cdot \Delta t < Q_{max} \quad (15)$$

Here Q_{min} is the minimum operational capacity, Q_{actual} is the present capacity, Δt is the time step and Q_{max} is maximum operational capacity. In option b) the voltage does not exceed the maximum (voltage control) by securing the following balance:

$$V_{t,min} < V_{oc} + I \cdot R < V_{t,max} \quad (16)$$

Here $V_{t,min}$ is the minimum terminal voltage, V_{oc} the open circuit voltage, I the current, R the internal resistance and $V_{t,max}$ the maximum terminal voltage.

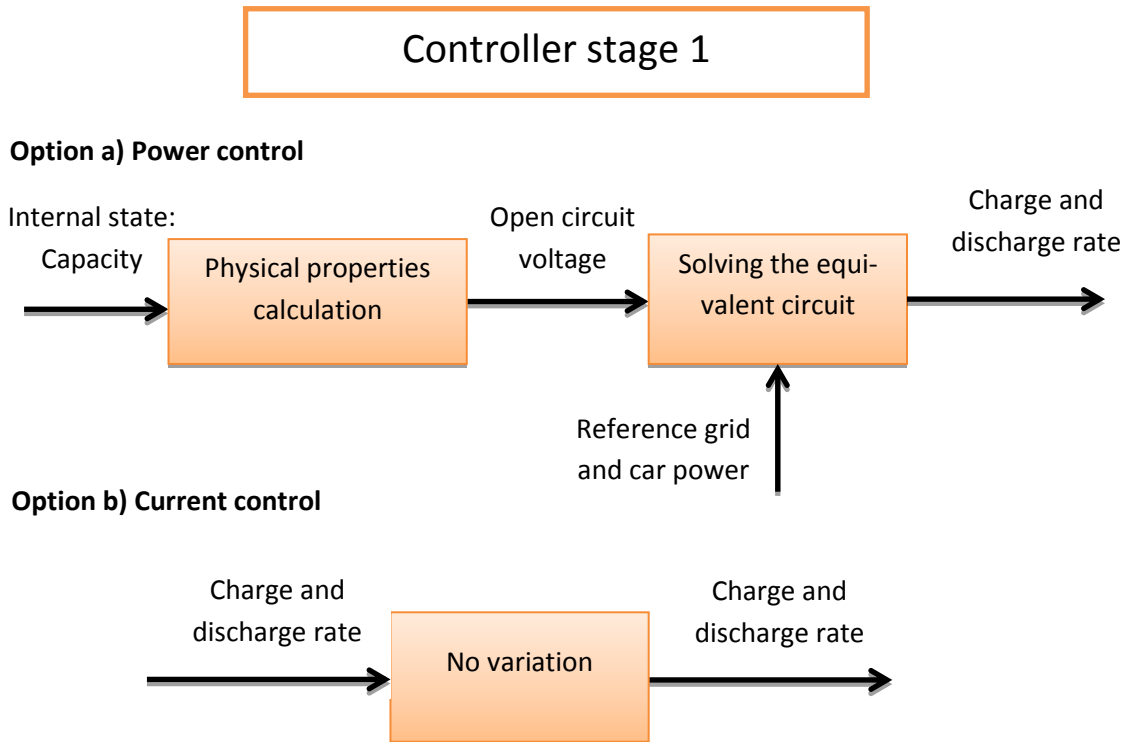


Figure 13: Layout of the controller stage 1

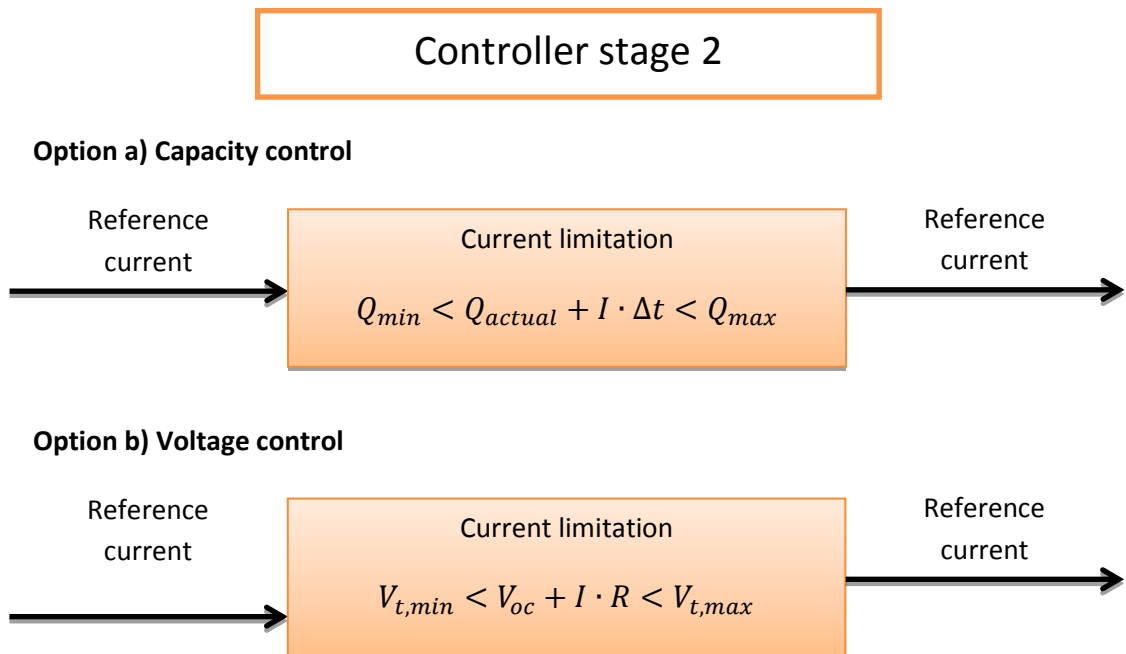


Figure 14: Controller stage 2

4.3.3. Solving the Equivalent Circuit

An important part of the control stage 1 option a) is determining the battery current for the equivalent circuit. The two basic equations that follow from the chosen equivalent circuit are

$$V_{bat} = V_{oc} + I_{bat} \cdot R_i \quad (17)$$

and

$$-P_{bat} = I_{bat} \cdot V_{bat} \quad (18)$$

where V_{bat} is the battery voltage, V_{oc} is the OCV, I_{bat} is the battery current, R_i is the internal resistance and P_{bat} is the battery power. The reason why the power is negative results from the definition of the power flow and the current flow. Solving (18) for V_{bat} and inserting in (17) V_{bat} and rearranging leads to the quadratic function:

$$0 = R_i \cdot I_{bat}^2 + V_{oc} \cdot I_{bat} + P_{bat} \quad (19)$$

Developing the equation further leads to the following two equations

$$\left(I_{bat} + \frac{V_{oc}}{2 \cdot R_i} \right)^2 = \frac{V_{oc}^2 - 4 \cdot R_i \cdot (P_{bat})}{4 \cdot R_i^2} \quad (20)$$

$$I_{bat; 1,2} = \frac{-V_{oc} \pm \sqrt{V_{oc}^2 - 4 \cdot (P_{bat}) \cdot R_i}}{2 \cdot R_i} \quad (21)$$

Problematic here is that the quadratic function can have either two, one or no solution. This can cause problems in the simulation and therefore suitable measures have to be taken so that the algorithm produces valid results. From left side of equation (20) follow two cases. The first case occurs during battery charging with $I_{bat} > 0$ and $P_{bat} < 0$. Here the expression inside the brackets becomes positive. When the open circuit voltage and the resistance is positive and the battery power is negative during charging, also the right side of the equation becomes positive. This allows the conclusion that only one solution for I_{bat} is valid and it must be positive in this case. The result with I_{bat} being negative can be ignored. The second case occurs during discharge with $I_{bat} < 0$ and $P_{bat} > 0$. Here the equation has no real solution for $P_{bat} > \frac{V_{oc}^2}{4 \cdot R_i}$. In order to avoid simulation inconsistencies the maximum battery power is set to $P_{bat} = \frac{V_{oc}^2}{4 \cdot R_i}$ so that the root does not become negative. Testing the algorithm revealed that there is only one valid solution for the quadratic function. In the algorithm this is considered by disregarding the second mathematical solution. The result is visualized in Figure 15. It can be seen that for high powers as an input (power requested) the allowed output power is reduced.

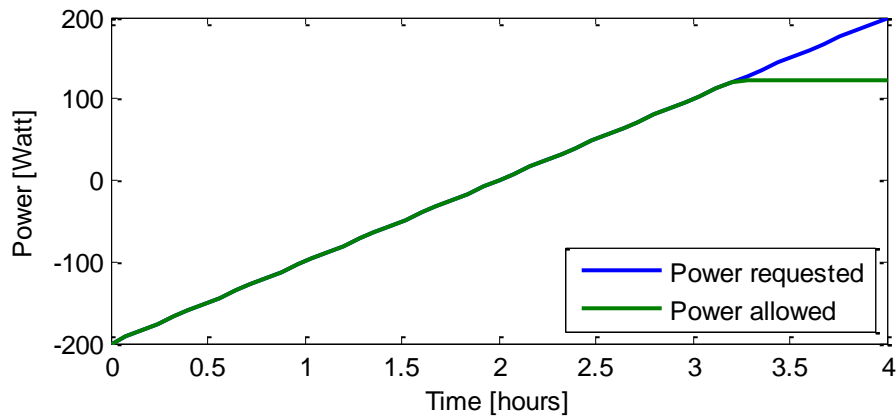


Figure 15: The limitation of the power for solving the equivalent circuit.

4.4. Power Allocation

The equipment connected to the HV OSS is visualized in Figure 16. The power flow is defined towards the OSS. Power flowing towards the charger, the battery, the electrical machine and auxiliaries is negative. The sum of all power flows are zero:

$$P_{charger} + P_{bat} + P_{aux,em} = 0 \quad (22)$$

where $P_{charger}$ is the charger power, P_{bat} is the battery power and $P_{aux,em}$ is the power of the auxiliaries and the electrical machine. Power flows towards the charger during V2G, to the electrical machine during regenerative braking, and to the battery during charging. Both directions for all three power flows are considered and implemented in the simulation.

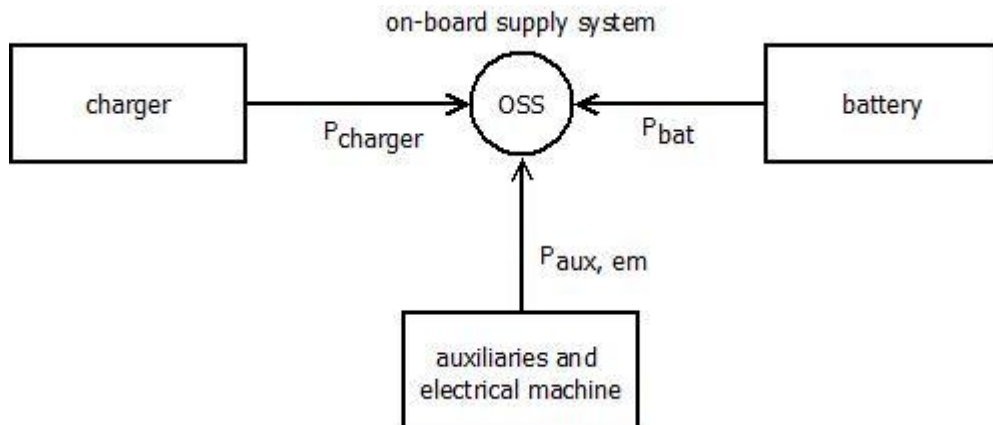


Figure 16: Definition of the power flows

The idea is that for each time step the average behaviour of all the components is modelled. This means that also a situation has to be considered where both charging and driving can occur. So in the simulation it may happen that power required for the car occurs at the same time as the power from the grid. The battery will not always be able to meet the request for example when the battery is almost empty. In this case the battery power has to be allocated to the car and the grid. Both requests from the grid and the car are given the same priority. Naturally also the power can be exchanged directly between the grid and the car auxiliaries

and electrical machine via the charger and the OSS. The condition that the absolute battery power is higher than the charger and the car power is not possible, due to the architecture of the control.

5. Verification and Results

The most important criterion for the assessment of the quality of a model is the convergence of the simulation with the behaviour of the simulated object in reality. Inconsistencies may origin from mathematically induced errors, due to modelling architecture, and effects that are not taken into account. In order to eliminate coding errors, the following methodology is used:

The model and its subsystems are tested systematically, using the two-step clear-box testing approach. A white box test ensures that every single path of the code returns an expected solution (either a result or an assertion). For complex models the code can also be translated into a flow chart, determining the paths that the program can follow, and finally analysing if expected results are obtained in each of the paths. Black box testing ensures that the outputs of a code are as expected, but in contrast to the white box testing, the analysis is completed with no knowledge of the inner code structure. For this examination the code is run for several numbers of input groups and the result must always be as expected. The code should be tested for the full range of values that have been set as the boundary conditions.

For testing the model assumptions, the general procedure is to first separate the testing for steady and transient state. Then, each module is verified independently and finally the model can be analysed as a whole. The test procedures necessary to confirm the validity depend on the nature of the model (phenomenological, physical or hybrid) and on the model requirements. The testing itself is not part of the thesis and will be carried out as consecutive projects.

5.1. Verification of the Battery Model

Figure 17 represents the validation of the battery cell voltage during operation with constant discharge current of a) 1.06 A (0.2 C), b) 2.65 A (0.5 C), c) 5.3 A (1 C), d) 7.95 A (1.5 C) and e) 10.6 A (2 C). The datasheet information is compared with the results of the model. When looking at the diagram, it can be observed that for every current the error reaches its maximum for a SOC of 0 %. The reason for the difference are the assumptions for the OCV and the resistance. The OCV is assumed to be the average between the discharge curve and the charging curve for a current equivalent to 0.7 C. The resistance is an average over the SOC window range (Chapter 4.3.1).

When looking at the worst case, for a discharge rate of 1 C the error is 15 % or 0.5 V. Considering that the SOC for each cell is between 20 % (1.06 Ah) and 80 % (4.24 Ah), the maximum error is much lower. Here, the worst case occurs for a medium discharge rate of 0.5 C and a capacity of 1.06 Ah. The maximum error amounts to 2 % (Figure 17 b). For low currents (Figure 17 a) the model shows a higher voltage than the curve of the datasheet. For high currents (Figure 17 e) the opposite is the case. The model curve is on average beneath the datasheet curve.

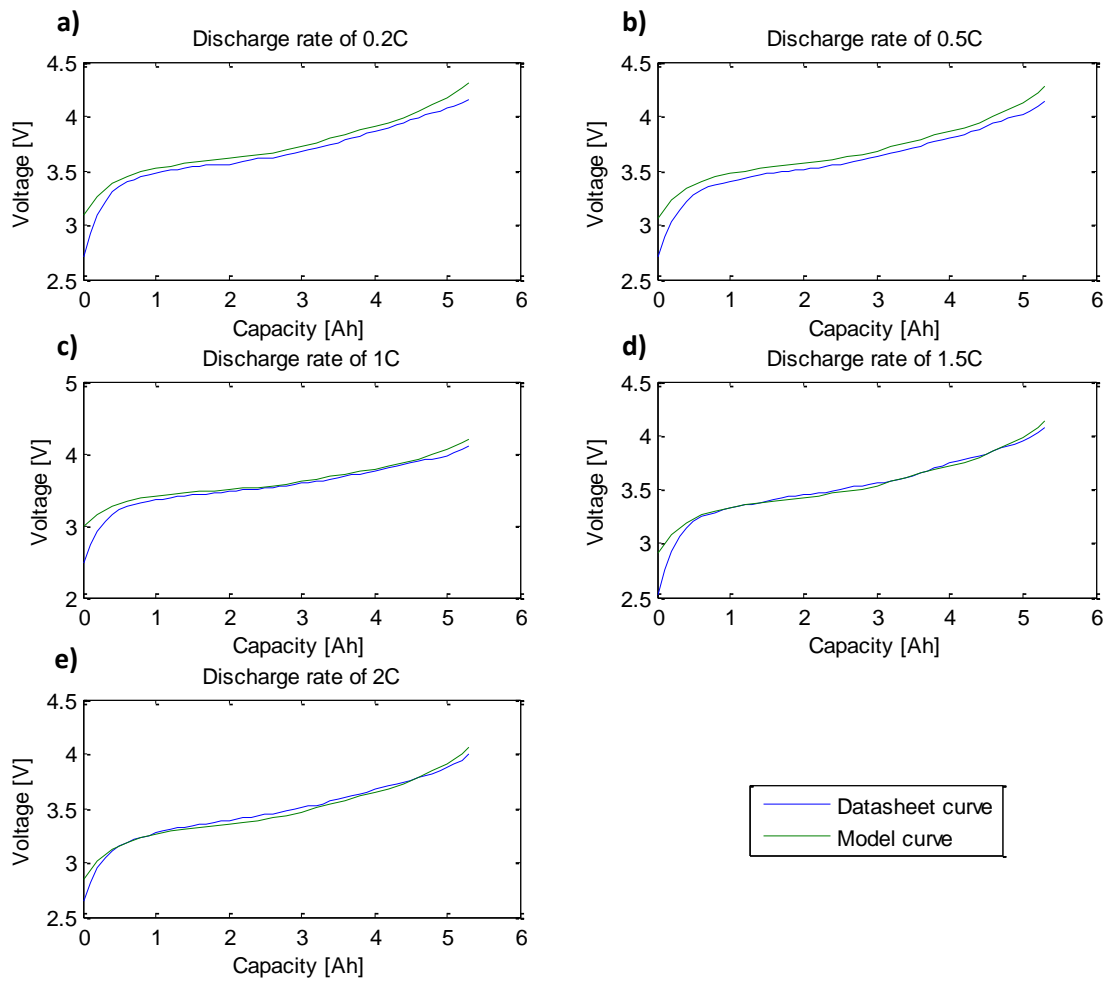


Figure 17: Discharging behaviour of the model compared with datasheet information

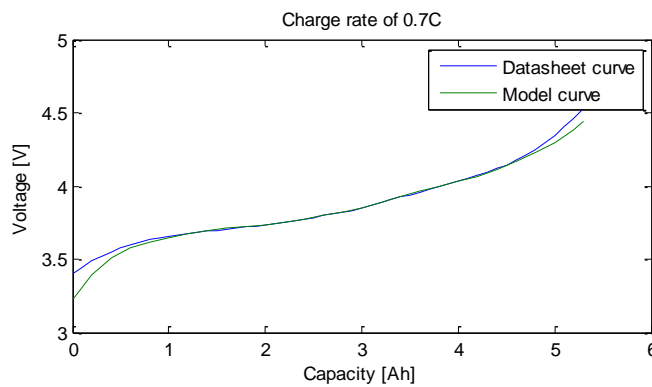


Figure 18: Charging behaviour of the model compared with datasheet information

During charging the model shows an almost perfect accuracy for errors less than 0.03 % in the SOC window of 20 % and 80 %. For an SOC of 0 % the error is higher and amounts up to 5 % (Figure 18). This result is expected because the curve was used for parameterization. Of interest would be other charging curves for the examination of the quality of the model.

5.2. Verification of the Control Strategies

The tool is set up for the support of different open loop control strategies. These control strategies are tested for their applicability and performance. The difference between them is the reference input, which is either a variable power or a constant current. Also the control strategies differentiate in how the SOC is limited during charging and discharging. In one case the charging current is reduced, so that it converges to a predefined capacity. In the second case the current is controlled, so that it converges to a certain voltage.

In industry voltage control is applied because Coulomb counting is more complex in the implementation. This has two practical reasons. The first is that measuring the voltage is simpler than measuring the current and integrating it over time. The second reason is that inefficiencies, leakages and self-discharge cause deviations of the real and the counted capacity. This error increases over time if it is not set back regularly. However, it is a useful and simple control that can be used for simulations.

Standard for most vehicles is CCCV control which is known as uncontrolled charging and is also implemented in this tool. The reason for choosing open loop control is that it allows long simulation time steps in the simulation.

5.2.1. Controller Stage 1: Power and Current Control

The power control which is used for V2G and to manage the power that is exchanged with the grid is the option a) for the controller stage one. The results and the response are depicted in Figure 19. It can be observed that the grid power varies and drops under 0 (V2G). For better visibility the actual grid power was lifted by 0.5 kW because the two curves match. The fact that they match is expected because there is no delay considered for the battery charger. Also there are no disturbances considered that influence the actual grid power.

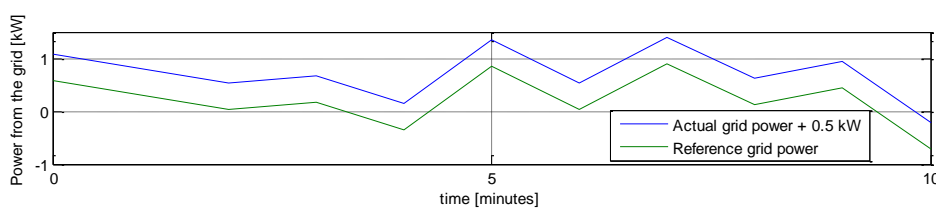


Figure 19: Behaviour of system for variable power control

The second option b) is to set the reference current directly which makes developing an algorithm for the first stage unnecessary. Also here V2G application can be tested, but in this case a constant current was assumed. The result is depicted in Figure 20 with a slightly rising power which corresponds to the rise in voltage. Although the actual grid power and the terminal voltage show a similar behavior, the changing efficiencies of the transmission and the charger cause a non-proportional relationship. Combined with the constant voltage control (Chapter 5.2.2), this control strategy represents the so called uncontrolled charging for EVs (CCCV).

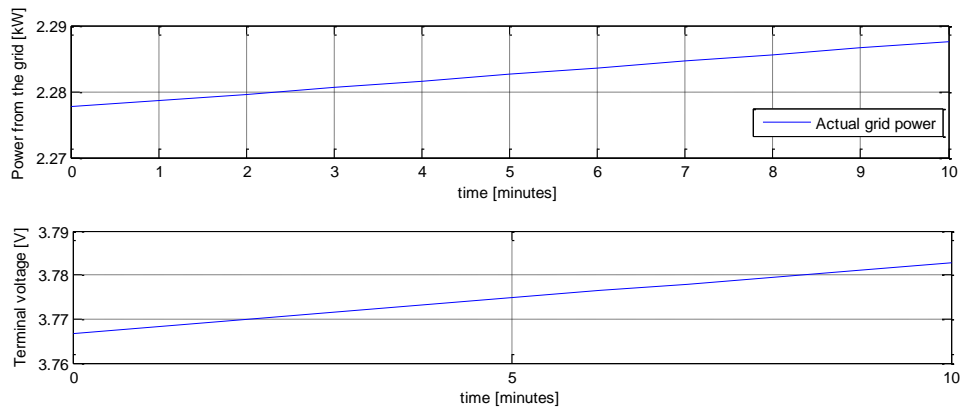


Figure 20: Behaviour of the system for a constant current of 0.53 A (0.1C)

5.2.2. Controller Stage 2: Capacity and Voltage Control

Also for the second stage there are two options implemented. The first one is based on the capacity of the battery. Before reaching the upper or lower boundary the algorithm reduces the current, so that the capacity converges to its maximum (Figure 21 a). The terminal voltage decreases, once the current drops (Figure 21 b and c). As a result, also the battery power converges to zero (Figure 21 d). For the simulation a constant current of 0.53 A as a reference input and a sample time of 1 minute was assumed. For lower sample times the response time is even shorter.

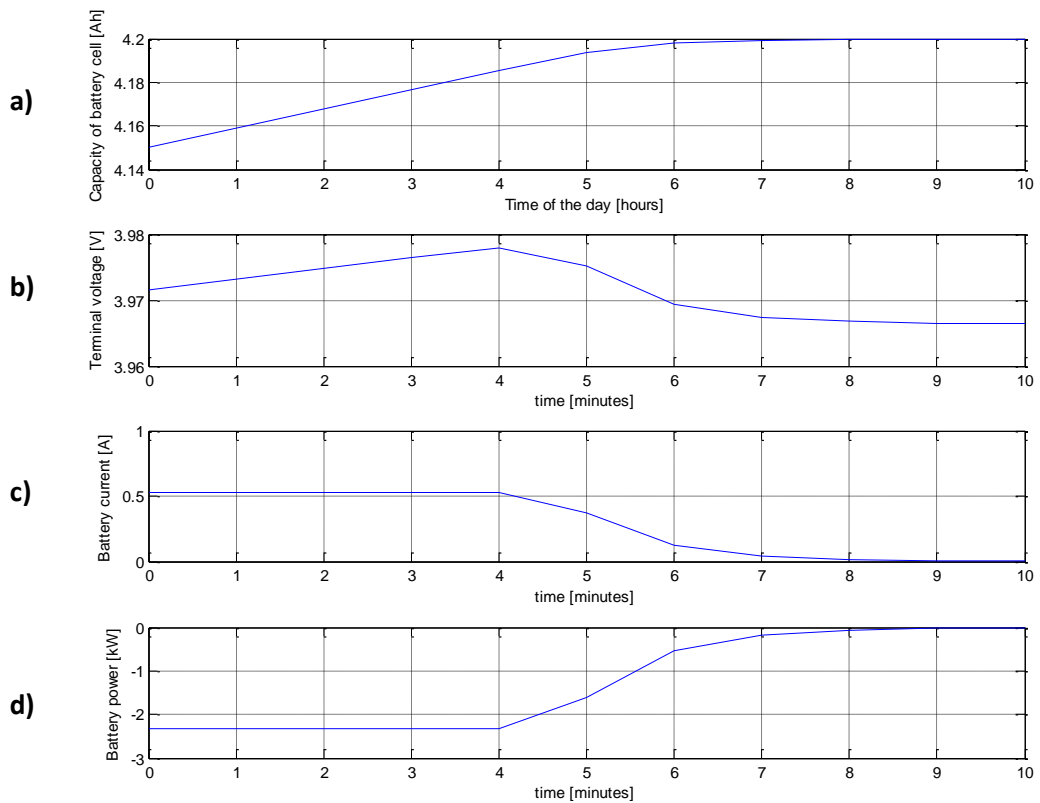


Figure 21: Behaviour of the battery for the controller stage 2 based on capacity

The second option is called voltage control. Also here the current is controlled, so that the voltage remains within the upper and lower boundary. For the verification charging to a maxi-

imum voltage of 4 V was simulated. The battery current drops to zero as well as the power once the upper voltage limit is reached (Figure 22). Also here the current is 0.53 A and the sample time is 1 minute.

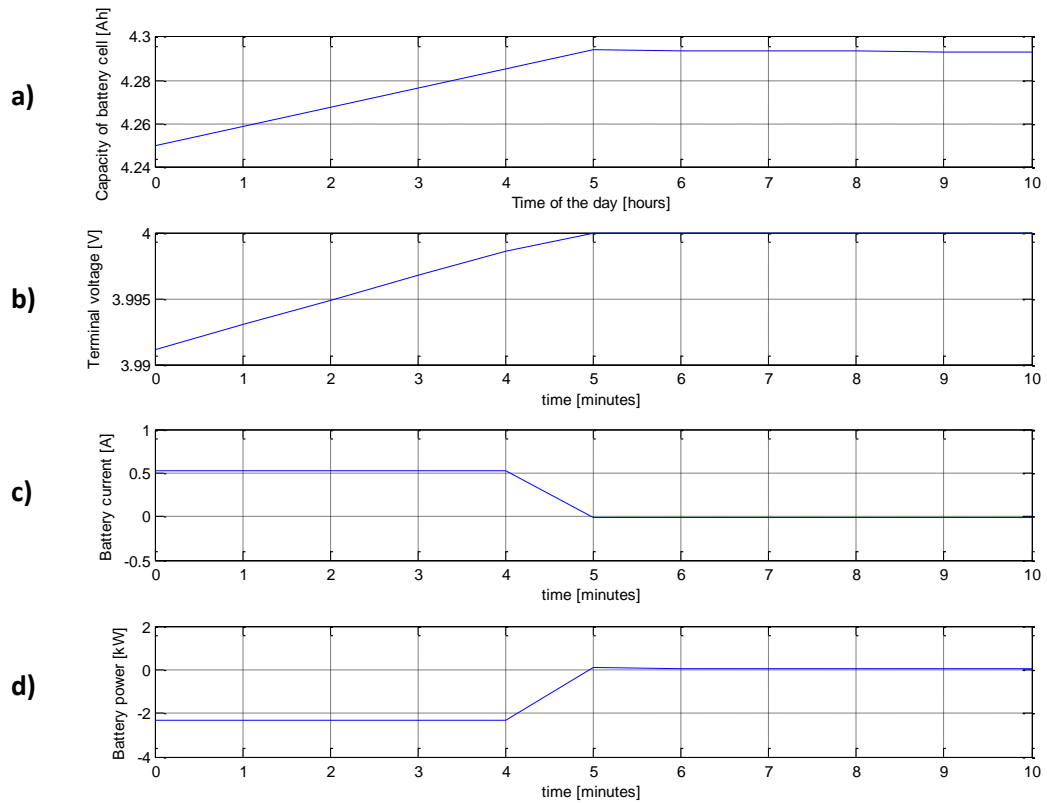


Figure 22: Behaviour of the battery for the controller stage 2 based on voltage

5.3. Test Case

In order to test the electric performance of an AEV, a simulation was carried out. The usable energy capacity is assumed to be 15.9 kWh and the simulated period is a one day starting at midnight. As a control strategy, constant current with coulomb counting and a sample time of one second was chosen. The assumptions are the following:

Infrastructure and charger

- Grid voltage of 230 V (phase to neutral) and a $\cos(\phi)$ of 1
- Cable length of 20 meters between the charging station and the house connection box with a cross section of 10 mm^2 and a relative resistance for copper of $1.678 \cdot 10^{-2} \frac{\Omega \cdot \text{mm}^2}{\text{m}}$
- Charging cable length of 5 meters [9] and a copper cable with a cross section of 10 mm^2
- Single phase mode 2 charging with a maximum power of 3.7 kW
- Charger with a capacity of 3 kW similar to Mitsubishi I Miev [27] and Smart for two (Source: Flinkster car sharing)

Battery

- 100 cells in series resulting in a nominal voltage of 365 V (Voltage level between 300 V and 500 V according to [2])
- 11 cells in parallel resulting and a usable energy capacity of 15.9 kWh which is similar to the energy capacity of Smart for two (16.5 kWh [28]), and Mitsubishi I Miev¹ (16 kWh [29])
- Characteristic of the Boston power Li-ion cell with a rated capacity per cell of 5.3 Ah [24]
- Minimum amount of charge of 1.06 Ah and a maximum amount of charge of 4.24 Ah per cell resulting in a nominal energy capacity of 21.23 kWh
- An initial SOC of 1 equivalent to a capacity of 4.24 Ah per cell

Vehicle

- Electricity consumption of 0.2 kWh/km including auxiliaries [30]

As operational parameters, the velocity profile in Figure 23 (a) was set. It represents a typical dynamic profile for a car that is used inside the city for a service company. Together with the constant specific electricity consumption per km the car power is proportional to the speed. During the period of 24 hours, the car is used 4 times which can be seen as a use case for a cost effective operation of an electric vehicle. The power availability is depicted in Figure 24 (a). The basis for this curve is a maximum grid power of 3.7 kW and an availability of the charging station at three periods of the day (from 03:10 to 08:20, 12:15 to 18:00, 19:00 to 23:10). For the simulation fixed time steps of one second are used. The vehicle speed data has a resolution of one second as well.

Number of journey / charging period	Travel distance	Final SOC _{window}	Charging time	Grid energy demand
1	42.5 km	35.2 %	3 hours and 3 minutes	9.09 kWh
2	18.0 km	73.19 %	1 hour and 17 minutes	3.86 kWh
3	25.3 km	62.1 %	1 hour and 48 minutes	5.42 kWh
4	17.7 km	73.8 %	-	-

Table 7: Summary of the test case simulation

Considering the assumptions made and the parameters that were set, the simulation shows interesting results for the performance of the electric vehicle (Figure 23). The vehicle drives a total amount of 103.5 km and requires 18.37 kWh from the grid. After each journey, the vehicle can be fully charged. The power from the grid amounts to 3.009 kW including losses of the transmission of 9 W.

¹ The Mitsubishi I Miev is also called Peugeot iOn, Citroën C-Zero and Mitsuoka Like (LWB)

Figure 23 e) shows the SOC_{window} during operation. It represents the SOC based on the difference in capacity between the maximum and minimum operational amount of charge (Chapter 2.2). Considering the values after the third charging process, where the battery recovers to a SOC_{window} of 1, conclusions for the performance of the charging system can be drawn.

The specific electricity consumption at the grid is 0.214 kWh/km. Recalling that the electricity consumption from the battery for propulsion and auxiliaries was assumed to be 0.2 kWh/km, this results in energy efficiency of the charging process of 93.45 % (including 97.9 % for the battery, 95.5 % for the charger and 100.0% for the transmission). The SOC_{window} drops to 35.2 % for the first journey, to 73.19 % for the second, 62.1 % for the third, and to 73.8 % for the fourth journey. For the use case this means that a successful operation in terms of battery capacity can be realized. Also fully charging the EV after each journey is possible. Without charging the battery it is empty after 64.2 km, so in theory there is no necessity for the second charging process. In total it takes about 5 hours and 30 min to fully charge the battery from an empty state.

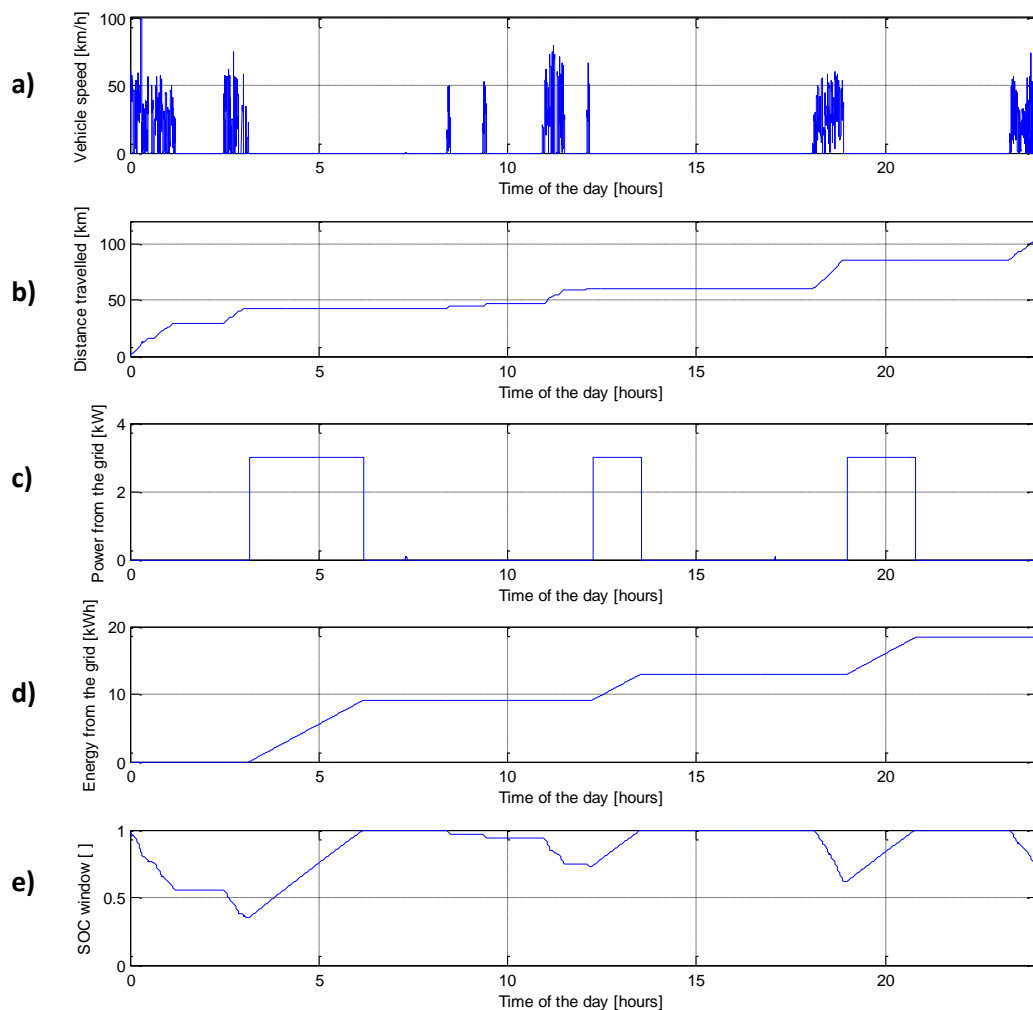


Figure 23: Performance of the EV

The internal states of the battery can be observed in Figure 24. The first plot shows the grid power that is available in theory during the charging process as well as the power that is actu-

ally used. Both curves indicate that the full power is used immediately after the vehicle arrives at the charging station. Also they illustrate that the charging process stops after 3 hours and 17 minutes with a buffer of about 2 hours until the next journey starts. Hence, there is potential to either reduce the charging power or to delay the charging process.

The vehicle power demand which is proportional to the vehicle speed is shown in the second plot. The power is negative because all the electricity flowing towards the OSS is defined to be positive. The terminal voltage per cell varies between 3.59 V and 4 V and the current between 0.71 A (charging) and -4.96 A (discharging) per cell. The battery power at the OSS varies between 20.5 kW (discharging) and -2.9 kW (charging).

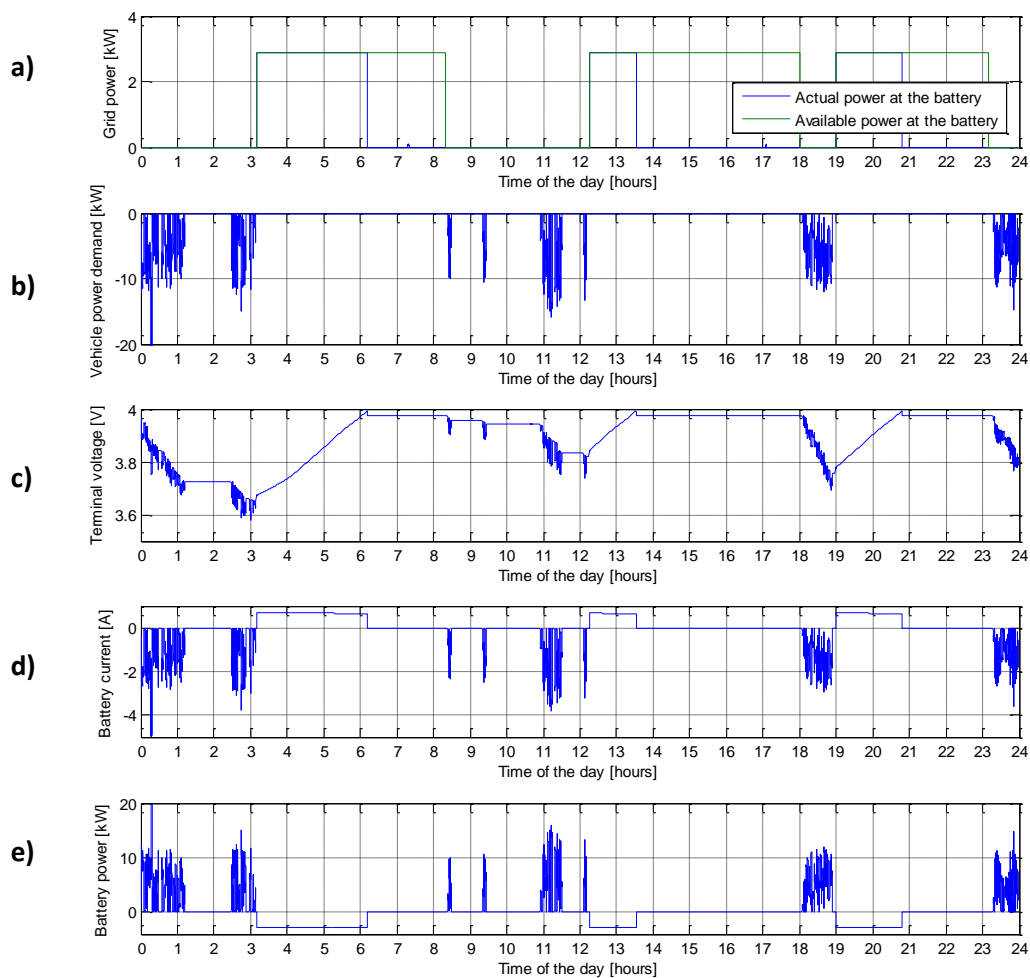


Figure 24: Internal states of the model for the test case

5.4. Review of the simulation tool

The test case has shown that the tool is able to describe the major variables involved in the charging and discharging process of an EV. The accuracy of the complete tool depends heavily on the assumption for the specific power consumption per km. For the battery the only effect modelled is the charge and discharge rate during a cycle. Other effects as described in Chapter 2.2 are not considered.

As a guideline the test case demonstrates the methodology for parameterizing the model. Together with the explanations in the previous chapters the characterization of the components becomes simple and allows users a quick understanding of the tool. All the information needed is based on datasheets, on publications or input from the industry and can be freely used. The methodology avoids measurements for parameterisation of the battery and other components. However, measurements are seen as a possibility to improve accuracy.

Further low simulation times are achieved. The elapsed time for a simulation with a time step of 1 minute and simulation of one day takes typically about 1.6 seconds. For the simulation a standard processor with 3.4 GHz, a random access memory of 4 GB and a 64 bit operating system was employed. The sample time and the simulation period can be adjusted to serve different study purposes.

The tool permits testing different energy management strategies that improve energy efficiency, energy availability, and battery aging by controlling the CR to the battery during charging. Limiting the CR causes a reduction in temperature of the battery and an in general an extension of the lifetime. However, a quantification of the aging process is not possible. For analysing the charging infrastructure the tool incorporates cable losses and charging modes. This allows researching the effect on the charging process in terms of time required and resulting efficiency. In addition the tool is implemented as a referenced model in Matlab/Simulink which permits the investigation of a fleet of EVs with the same underlying model but with altered parameters. In terms of universality the allocation of power allows a bidirectional flow of battery, car and grid power which simulates regenerative braking and V2G operation.

For the analysis of different charging processes a useful feature is the control system. Both uncontrolled charging as well as controlled charging with variable grid power is implemented. As a result it is possible to study an EV as a controllable load for an optimal dispatch of the available electric power in a smart grid.

6. Conclusion

The tool developed in the thesis contains a model of the electric vehicle and the charging infrastructure, as well as a control algorithm. It allows the simulation of an electric vehicle including driving and charging and is optimized for low computational effort and wide applicability. The simulation takes 2 seconds for one day with a sample time of one minute on a standard computer. The battery is modelled as an equivalent electric circuit with a variable open circuit voltage in series with a constant resistance. The charger is characterized by an ideal response time and a power dependent efficiency. The losses of the transmission are composed of the charging cable and the cord to the house connection box. Defining parameters of the respective models allows the simulation of various designs and operational conditions.

A review of different battery models showed that simple equivalent circuit battery models are the only option for an application in the presented simulation tool. They require low parameterization effort, are based on generic information, and have low computational time. More sophisticated equivalent circuit models need measurements, and physical models involve knowledge of the composition, as well as complex calculations. Accordingly, a battery modeling approach for EVs is implemented that fulfils all requirements. It is based on an electric circuit and considers the performance for different CRs. For the applied battery the voltage error is less than 2 % when comparing with information provided in a data sheet.

The main performance indicators for batteries are energy efficiency and energy capacity. High temperatures and high current rates have negative consequences as well as discharge to low DODs and large number of cycles. These operational parameters can be differentiated between having short and long term as well as reversible and irreversible effects. The findings are that (a) low temperature strongly affects the charging/discharging capability and the available energy of a battery, (b) high temperatures and full DOD accelerate the energy fade and shorten the battery lifetime, and (c) high current rates decrease energy efficiency and shorten the battery lifetime for both charging and discharging.

The main components that cause losses during charging are presented and found to be the charger (around 93 %) and the battery (around 95 %). The auxiliaries are found to have a strong impact on the EV performance. They require an average of approximately 2.47 kW and can cause a quick depletion of the battery due to thermal conditioning.

The implemented control mimics the behaviour of a real charger. No feedback loop is implemented due to simulation sample times of up to 1 minute. Rather, a two stage open loop control enables simulations of controlled and uncontrolled charging (CCCV). The first stage determines the current rate and the second stage limits the current to the SOC window. As a reference input for the control the grid power or the current is set.

In a test case, an EV with similar parameters to the Mitsubishi iMiev and a typical charging process is simulated. A dynamic velocity profile was chosen resulting in a specific grid electricity consumption of 0.214 kWh/km. The energy efficiency is 97.9 % for the battery, 95.5 % for

the charger and 100.0% for the transmission resulting in a total efficiency of 93.5 %. A total distance of 64.2 km is the maximum value for an EV with a battery energy capacity of 15.9 kWh.

6.1. Further Work

It is evident that the integration of EVs requires further research and development on both the grid and the vehicle level. Here the tool can be used to investigate current research topics such as energy management strategies, vehicle fleet operation, and thermal preconditioning.

As a continuation of the project further research on both the electric vehicle and certain components such as the battery are highly recommendable. The review of different battery models has shown that battery characterization is a key for understanding the complex interconnected effects that influence battery performance. Furthermore, sophisticated models allow the incorporation of more characteristics that influence battery performance parameters such as temperature. A first step could be the expansion of the battery model by considering the thermal behaviour. A common approach is presented in [14]. This also enables long term characterization of batteries and incorporation of aging models.

In the tool a constant value for the electricity consumption per km was used. This assumption can be avoided by modelling the demand dynamically. Here the consideration of acceleration, recuperation, and losses will improve the model noticeably. As a verification of the model, the messages that are transmitted via the CAN-bus contain useful information about the state of the vehicle. It is possible to read this data using commercial measurement technology. Conclusions can be drawn in terms of:

- energy and cycle efficiency
- charger efficiency
- battery temperature level
- battery terminal voltage level
- storable energy at different temperature levels
- electricity demand of auxiliaries
- power limitations of the charger

From the perspective of the industry, this work sets the basis for service and product development. In particular, virtual power plant operators and distribution system operators require simple simulation tools that can be applied in the control of an energy management system. Implemented in a SCADA (Supervisory Control And Data Acquisition) system, the algorithms can help organize generation, storage, and demand. They can also control electric vehicles.

Furthermore, the tool can be used for demand forecast of electric vehicle charging stations because it can generate a profile that varies with the design of the EV, the charging station, and the control strategy. For vehicle fleet operators, this tool can help test the application of EVs as an alternative to conventional cars, as well as estimate the distance an EV can travel and charging times according to different charging modes. In conclusion, the algorithm pre-

sented above offers a promising and effective methodology with which to model and predict the performance of electric vehicles in society.

References

- [1] European Commission, "Road transport: Reducing CO₂ emissions from vehicles," 2012. [Online]. Available: http://ec.europa.eu/clima/policies/transport/vehicles/index_en.htm. [Accessed: 26-Apr-2013].
- [2] S. F. Tie and C. W. Tan, "A review of energy sources and energy management system in electric vehicles," *Renewable and Sustainable Energy Reviews*, vol. 20, pp. 82–102, Apr. 2013.
- [3] A.T. Kearney Global Powertrain Team, "Powertrain 2025-A global study on the passenger car powertrain market towards 2025," 2012. [Online]. Available: http://www.atkearney.de/documents/856314/1214682/BIP_Powertrain_2025.pdf/9db4b0fe-ea05-4df8-ab8b-8425d7d1f9a2. [Accessed: 05-Jul-2013].
- [4] F. Graf, F. Pellkofer, M. Wegerer, and J. Maiterth, "Plug-in Hybrid Architektur," *Automobiltechnische Zeitung (ATZ)*, pp. 406–411, 2013.
- [5] International Electrotechnical Commission, "International Standard 62196-1," 2004. [Online]. Available: http://www.iec-normen.de/dokumente/preview-pdf/info_iec62196-1{ed1.0}b.pdf. [Accessed: 05-Jul-2013].
- [6] Forschungsstelle für Energiewirtschaft e.V. (fE), "Endbericht Batteriemessungen AZE," 2012.
- [7] C. F. Eckhardt, E. Lindwedel, K. Gödderz, M. Vivian, M. Schwarz, C. Hufnagl, G. Nissen, U. Schulte, D. Jin, and T. Stöhr, "Gesteuertes Laden V2.0," 2011.
- [8] Mennekes Elektrotechnik GmbH & Co. KG, "Medieninformation," 2011. [Online]. Available: http://int.mennekes-website.de/uploads/media/MENNEKES_Medieninformation_-_Ladestecker-Standards_in_der_IEC_Norm_02.pdf. [Accessed: 05-Jul-2013].
- [9] MENNEKES Elektrotechnik GmbH & Co. KG, "Ladesysteme für Elektrofahrzeuge," 2012. [Online]. Available: http://www.mennekes.de/uploads/media/MENNEKES_-_Elektromobilitaet_-_D_2012_2.pdf. [Accessed: 05-Jul-2013].
- [10] BDEW Bundesverband der Energie- und Wasserwirtschaft e.V., "Technische Anschlussbedingungen TAB 2007." 2007.
- [11] F. Marra, C. Traholt, E. Larsen, and Q. Wu, "Average behavior of battery-electric vehicles for distributed energy studies," in *2010 IEEE PES Innovative Smart Grid Technologies Conference Europe (ISGT Europe)*, 2010, pp. 1–7.
- [12] P. Ramadass, B. Haran, R. White, and B. N. Popov, "Mathematical modeling of the capacity fade of Li-ion cells," *Journal of Power Sources*, vol. 123, no. 2, pp. 230–240, Sep. 2003.

- [13] K. A. Böhm, *Charakterisierung und Modellierung von elektrischen Energiespeichern für das Kfz*. Aachen, Germany: Shaker Verlag, 2008.
- [14] S. H. Jensen, C. N. ; Rasmussen, and G. Yang, "Electric vehicles in a distributed and integrated market using sustainable energy and open Networks - Report work-package 1.5 Battery modelling," 2009.
- [15] "Boston Power Inc., Data sheet: Swing® 5300 Rechargeable Lithium-ion Cell." [Online]. Available: http://www.boston-power.com/sites/default/files/documents/940-0013-001_Swing_5300_DS_Rev_001_0.pdf.
- [16] D. Haifeng, "A new SOH prediction concept for the power lithium-ion battery used on HEVs," *2009 IEEE Vehicle Power and Propulsion Conference*, pp. 1649–1653, Sep. 2009.
- [17] S. Amjad, S. Neelakrishnan, and R. Rudramoorthy, "Review of design considerations and technological challenges for successful development and deployment of plug-in hybrid electric vehicles," *Renewable and Sustainable Energy Reviews*, vol. 14, no. 3, pp. 1104–1110, Apr. 2010.
- [18] VDE Verband der Elektrotechnik Elektronik Informationstechnik E.V. Association for Electrical Electronic and Information Technologies, "Elektrofahrzeuge; Bedeutung Stand der Technik, Handlungsbedarf," 2010. [Online]. Available: <http://www.vde.com/de/fg/ETG/Arbeitsgebiete/Q6/Aktuelles/Oeffentlich/Seiten/VDE-StudieElektrofahrzeuge.aspx>. [Accessed: 05-Jul-2013].
- [19] M. Jung, A. Kemle, T. Strauss, and M. Wawzyniak, "Innenraumheizung von Hybrid-und Elektrofahrzeugen," *Automobiltechnische Zeitung (ATZ)*, pp. 396–402, 2011.
- [20] M. Yilmaz and P. T. Krein, "Review of Battery Charger Topologies, Charging Power Levels, and Infrastructure for Plug-In Electric and Hybrid Vehicles," *Power Electronics, IEEE Transactions on*, vol. 28, no. 5. pp. 2151–2169, 2013.
- [21] H. Turker, S. Bacha, D. Chatroux, and A. Hably, "Modelling of system components for Vehicle-to-Grid (V2G) and Vehicle-to-Home (V2H) applications with Plug-in Hybrid Electric Vehicles (PHEVs)," in *Innovative Smart Grid Technologies (ISGT), 2012 IEEE PES : Innovative Smart Grid Technologies (ISGT), 2012 IEEE PES*, 2012, pp. 1–8 TS – RIS.
- [22] F. Marra, G. Yang, and C. Traholt, "Demand profile study of battery electric vehicle under different charging options," *Power and Energy Society General Meeting 2011 IEEE*, pp. 1–7, 2012.
- [23] J. Kowal, J. B. Gerschler, C. Schäper, T. Schoenen, and D. U. Sauer, "Efficient battery models for the design of EV drive trains," pp. 31–38, 2010.
- [24] J. V. Barreras, E. Schaltz, S. J. Andreasen, and T. Minko, "Datasheet-based modeling of Li-Ion batteries," *2012 IEEE Vehicle Power and Propulsion Conference*, pp. 830–835, Oct. 2012.

-
- [25] O. Tremblay, L.-A. Dessaint, and A.-I. Dekkiche, "A Generic Battery Model for the Dynamic Simulation of Hybrid Electric Vehicles," *2007 IEEE Vehicle Power and Propulsion Conference*, no. V, pp. 284–289, Sep. 2007.
- [26] H. Culcu, B. Verbrugge, N. Omar, P. Van Den Bossche, and J. Van Mierlo, "Internal resistance of cells of lithium battery modules with FreedomCAR model," *World Electric Vehicle Journal*, vol. 3, pp. 1–9, 2009.
- [27] ecodrive Ltd., "Mitsubishi i-MiEV." [Online]. Available: <http://www.ecodrive.co.uk/Mitsubishi-i-MiEV>. [Accessed: 27-Jun-2013].
- [28] Wikipedia, "Smart Fortwo." [Online]. Available: http://de.wikipedia.org/wiki/Smart_Fortwo. [Accessed: 27-Jun-2013].
- [29] Wikipedia, "Mitsubishi i-MiEV." [Online]. Available: https://en.wikipedia.org/wiki/Mitsubishi_i-MiEV. [Accessed: 27-Jun-2013].
- [30] International Energy Agency, "Technology Roadmap - Electric and plug-in hybrid electric vehicles," 2011. [Online]. Available: <http://www.iea.org/publications/freepublications/publication/name,3851,en.html>. [Accessed: 05-Jul-2013].

Appendix A: Glossary for the Term Capacity

In general, the capacity of a cell may refer to the amount of charge that can be charged, discharged or stored by the cell. Capacities are specified in the unit Ah and are the product of current and time. A discharge rate of 1C means that the battery is depleted in 1 h while 2C indicates that the battery is discharged in only half an hour. The different types of capacity are described below:

Nominal Capacity

The nominal capacity is known as the capacity of a cell, which can be discharged at nominal conditions (nominal current and nominal temperature) until a certain predefined minimum voltage is reached.

Removable capacity

The removable capacity is the amount of charge that can be discharged at any predefined power and temperature until the final discharge voltage of the cell is reached. Due to the arbitrariness of power and temperature, there is one value for each case.

Maximum available capacity

The maximum available capacity describes the amount of charge that can be removed from a fully charged cell. For a new cell the maximum available capacity is equal to the rated capacity. For used batteries the state of health (SOH, see below) is the mathematical representation of the age.

Capacity loss

The capacity loss refers to the phenomenon that a cell can store and release less capacity. The capacity loss can either be reversible (SOC) or irreversible (SOH).